Post-Caledonian tectonic evolution of the Precambrian and Palaeozoic Platforms boundary zone offshore Poland based on the new and vintage multi-channel reflection seismic data

Quang Nguyen[1], Michal Malinowski[1,2], Stanisław Mazur[3], Sergiy Stovba[3,4], Małgorzata Ponikowska[3], and Christian Hübscher[5]

[1] Institute of Geophysics, Polish Academy of Sciences, Warsaw, 01-452, Poland
[2] Geological Survey of Finland, Espoo, FI-02151, Finland
[3] Institute of Geological Sciences, Polish Academy of Sciences, Kraków, 31-002, Poland
[4] S.I. Subbotin Institute of Geophysics, National Academy of Sciences of Ukraine, Kyiv, 02000, Ukraine
[5] Institute of Geophysics, University of Hamburg, 20146, Hamburg

Correspondence to: Quang Nguyen (qnguyen@igf.edu.pl)

Abstract. The structure of the post-Caledonian sedimentary cover in the transition from the Precambrian to the Palaeozoic Platforms in the Polish sector of the Baltic Sea is a matter of ongoing debate, due to the sparsity of quality seismic data and insufficient well data. The new high-resolution BalTec seismic data acquired in 2016 contributed greatly to deciphering the regional geology of the area. Here we ~~develop~~show an optimal seismic data processing workflow for the selected new BalTec seismic profiles offshore Poland as well as legacy PGI97 regional seismic data. Due to the acquisition in a shallow water environment, the processing strategy focused on suppressing multiple reflections and guided waves, through a cascaded application of modern ~~SRME, τ-p deconvolution, water bottom F-K filtering, and parabolic Radon~~ multiple elimination approaches. ~~We also perform reprocessing of the legacy PGI97 regional seismic data, achieving significant improvement in overall data quality compared to the original processing.~~ We illustrate~~showcase~~ the potential of the new and reprocessed data focusing seismic interpretation on the area of the Koszalin Fault. In the light of the ~~data available~~ available data, the Koszalin Fault was the main structure controlling Mesozoic subsidence and Late Cretaceous-Paleocene inversion of the eastern portion of the Mid-Polish Trough offshore Poland. The inversion changed its character from thin- to thick-skinned towards the north, away from the Polish coast. The Koszalin Fault reactivated older structural grain inherited from the time of Devonian continental rifting at the margin of Laurussia. The fault runs obliquely to the ~~CDF~~ Caledonian Deformation Front, the feature that remained inactive since its formation at the Silurian-Devonian transition.

1 Introduction

The transition from the East European Platform to the Palaeozoic Platform of Western Europe has been for a long time a matter of lively discussion (e.g., Berthelsen, 1998; Pharaoh, 1999; Thybo, 2001; Bayer et al., 2002; Mazur et al., 2016; Janik et al., 2022; ~~Ponikowska et al., 2023~~ Ponikowska et al., 2024 and references therein). Besides the Teisseyre-Tornquist Zone (TTZ)

which is considered a boundary between the two platforms, there are additional structural elements that contribute to the complexity of the transition zone such as the Caledonian Deformation Front (CDF; Berthelsen, 1998; Katzung et al., 1993; Lassen et al., 2001; Krawczyk et al., 2002) or late Palaeozoic tectonic grabens (Krzywiec et al., 2022a). These features are particularly apparent in the southern Baltic Sea where the CDF diverges away from the TTZ (Fig. 1a~~A~~) and a mosaic of various geological blocks, separated by several fault zones, was formed throughout the late Palaeozoic and Mesozoic (e.g., Erlström et al., 1997; Seidel et al., 2018; ~~Ponikowska et al., 2023~~Ponikowska et al., 2024). These structures were produced by consecutive tectonic events including, among others, the emplacement of the Caledonian fold-and-thrust belt (e.g., Mazur et al., 2016); late Palaeozoic extension west of the TTZ (Krzywiec et al., 2022a), Mesozoic extension (e.g., Krzywiec et al., 2003; Mazur et al., 2005), and finally Late Cretaceous-Paleocene basin inversion (e.g., Krzywiec, 2002; Krzywiec et al., 2003, 2022b; Al Hseinat and Hübscher, 2017; Pan et al., 2022).

Seismic imaging remains the most effective tool for resolving the complexity of superimposed structural elements in the transition zone from the Precambrian to Palaeozoic Platforms in the southern Baltic Sea. However, sedimentary succession in the Polish sector of the southern Baltic Sea has been so far poorly explored by low-quality industry single-channel and multi-channel seismic (MCS) reflection profiles and a few boreholes (Pokorski, 2010; Jaworowski et al., 2010). The best regional coverage (both in Polish, but also German and Danish sectors) is offered by a high-resolution dataset acquired in 1996-97 in the southern Baltic Sea (PGI97, Kramarska et al., 1999). These data mostly document the shallow Cenozoic and Mesozoic sedimentary strata (down to 0.8 s TWT) and only in a few places reach the base of the Mesozoic (Krzywiec et al., 2003; 2002). Since the initial interpretation by Krzywiec et al. (2003), no attempts have been made to re-process and re-interpret these data. In March 2016, 3500 km of new MCS profiles were acquired onboard R/V Maria S. Merian ~~(see Hübscher et al., 2017)~~ throughout a large area of the Baltic Sea from the Bay of Kiel to the northeast of Bornholm (Hübscher et al., 2017; Hübscher, 2018) (cruise MSM52, also known as BalTec). Thanks to the unique acquisition parameters, the BalTec MCS data image the tectonic elements from the seafloor down to the Palaeozoic basement. With its large geographic coverage and resolution, these seismic data provide better capabilities for visualizing geological features and mapping structural formations than previous datasets (see examples of new interpretation, e.g. in Ahlrichs et al., 2020; Ahlrichs et al., 2022; Janik et al., 2022; Krzywiec et al., 2022b; Nguyen et al., 2023).

The aim of this contribution is twofold. First, we illustrate the efficiency of processing work for the newly acquired BalTec seismic data. ~~we showcase the development of the optimal seismic data processing workflow for the selected BalTec profiles offshore Poland. A lot of attention was paid to multiple reflection removal strategies for this kind of shallow water data.~~ Furthermore, we investigate if modern processing tools can improve the quality of the legacy PGI97 data and to what extent these data can supplement the interpretations derived from the BalTec profiles. Finally, with the newly processed and reprocessed data, we perform seismic interpretation to put some constraints on the structural pattern of sedimentary successions

in the transition zone from the Precambrian to Palaeozoic Platforms. The central part of the interpretation is the tectonic evolution of the Koszalin Fault and its relation to the CDF offshore Poland.
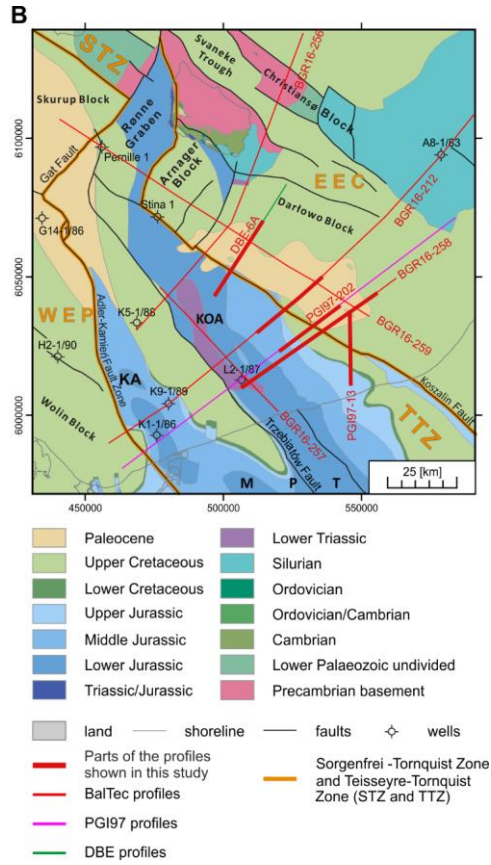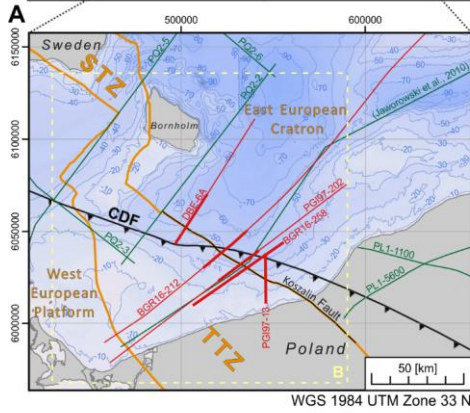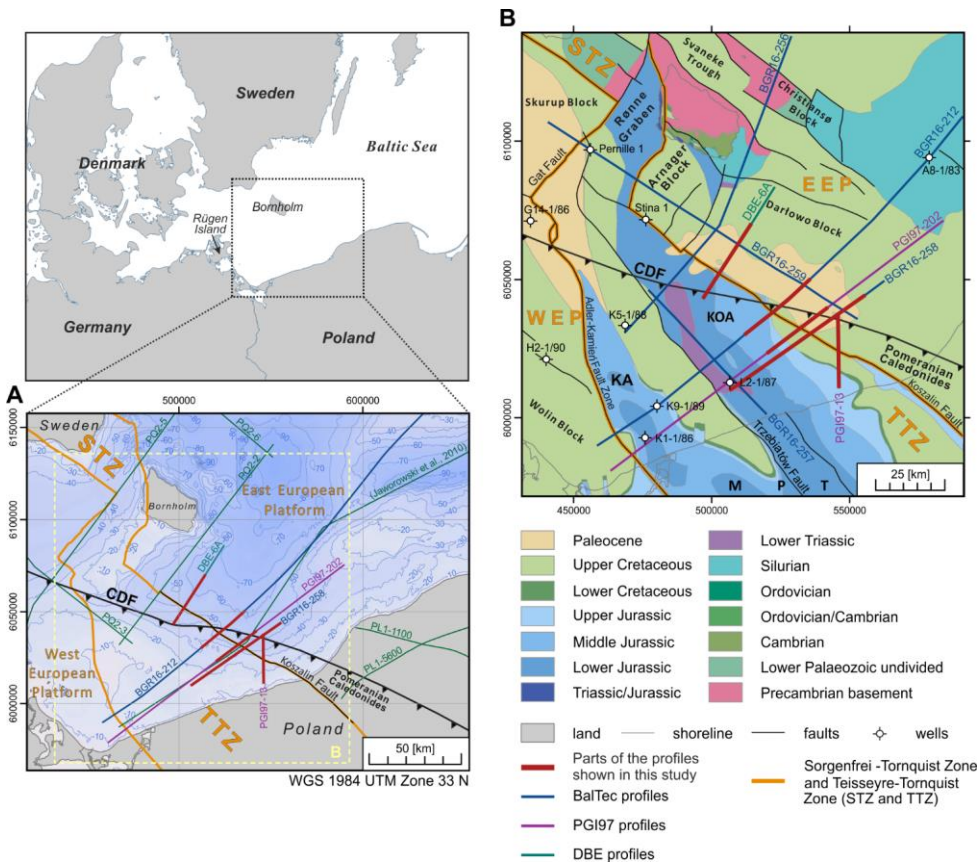
65

Figure 1: Location of the studied seismic profiles overlaid on main structural elements of the southern Baltic Sea. (aA) The bathymetry of the southern Baltic Sea and the location of seismic lines (red lines) were processed and shown in the study. Additionally, the location of the other deep seismic profiles from previous investigations: DEKORP-PQ (PQ2-2 to PQ2-6) in the offshore Bornholm (DEKORP-BASINResearch Group, 1999), regional cross-section from Jaworowski et al. (2010); and
PolandSPAN^TM PL1-1100 and PL1-5600 in onshore Poland (Mazur et al., 2015; 2016) are shown in green. (bB) Geological map of the southern Baltic Sea without post-Paleocene sediments after Kramarska et al. (1999), Schlüter et al. (1998), Sopher et al. (2016) and Pre-Quaternary map of Bornholm (Hansen and Poulsen, 1977). The position of main faults and tectonic blocks as well as the Teisseyre-Tornquist and Sorgenfrei-Tornquist Zones are adapted from Seidel et al. (2018). Abbreviations: CDF

– Caledonian Deformation Front; EEC – East European Craton; WEP – Western European Platform; KA – Kamień Anticline;

75 KOA – Kołobrzeg Anticline; MPT – Mid-Polish Trough; STZ – Sorgenfrei-Tornquist Zone; TTZ – Teisseyre-Tornquist Zone.

2 Geological background

The southern Baltic Sea area is located in the transition zone between the Fennoscandia Shield as part of the East European Craton (EEC) and the West European Platform (WEP). This area is characterized by a mosaic of various geological blocks separated by several faults and fault zones formed throughout the Phanerozoic (Liboriussen et al., 1987; Vejbaek et al., 1994;

80 Berthelsen, 1998; Pharaoh, 1999; Thybo, 1999; van Wees et al., 2000). The most prominent tectonic features are the NW-SE trending Sorgenfrei-Tornquist and Teisseyre-Tornquist Zones (STZ and TTZ), crossing the southern Baltic Sea to the north and south of Bornholm, respectively (Fig. 1aA; Berthelsen, 1998; Pharaoh, 1999). These zones are characterized by major, often deeply rooted faults that governed subsidence and uplift of major crustal blocks during several tectonic phases in the Palaeozoic, Mesozoic, and locally, Cenozoic (Vejbaek et al., 1994; Dadlez et al., 1995; Krzywiec et al., 2002, 2003).

85 At the southwestern margin of the EEC, Proterozoic granites and gneisses are overlain by Cambro-Ordovician sediments of the Baltica passive margin as penetrated by offshore wells (e.g., Franke et al., 1994; Beier and Katzung, 1999). The closure of the Tornquist Ocean and the subsequent collision of Baltica with Avalonia during the Late Ordovician led to the formation of the Caledonian fold and thrust belt (Katzung et al., 1993; Dallmeyer et al., 1999; Katzung, 2001; Torsvik and Rehnström, 2003). In this context, the Cambro-Ordovician successions of the Baltica margin were overthrust by deformed marine

90 Ordovician sediments (Katzung et al., 1993). The formation of an accretionary wedge is indicated by seismic surveys offshore Rügen Island (Babel Working Group, 1993; Thomas et al., 1993; Piske et al., 1994; Schlüter et al., 1997; DEKORP-BASINResearch Group, 1999). In addition, evidence of deformed Ordovician sediments of marine origin was found in several deep wells on Rügen Island (e.g., Dallmeyer et al., 1999; Katzung, 2001). The northernmost extension of the Caledonian fold and thrust belt is marked by the CDF, which can be traced from Lolland and Møn (Denmark) to the north of Rügen Island and

95 farther towards north-western Poland (Fig. 1aA; Liboriussen et al., 1987; Erlström et al., 1997). The CDF onshore NW Poland is marked out by a thin-skinned fold-and-thrust belt involving Ordovician and Silurian mudrock succession of the Pomeranian Caledonides (Mazur et al., 2016). The oldest sediments there are late Llanvirn and Caradoc in age and they are accompanied by fragments of the entire Silurian profile, up to the Pridoli (Podhalańska and Modliński, 2006). This is in contrast to the Rügen area, where only thick (~1500-2000 m) Ordovician sediments have been drilled (e.g., Katzung et al., 1993) including

100 Tremadoc–Llanvirn sandstones, shales and greywackes that experienced anchizonal metamorphic conditions (Dallmeyer et al., 1999). Therefore, the Pomeranian Caledonides with their potential offshore continuation are considered part of the Caledonian foreland basin that was deformed and included in the orogenic wedge during the late stages of Caledonian shortening (Mazur et al., 2016). Consequently, the CDF separates the undeformed succession of lower Palaeozoic sediments in the northeast, referred to as the Baltic Basin, from the Caledonian fold and thrust belt in the southwest (Fig. 1aA). The latter

105 forms the basement of the WEP that is unconformably covered by Devonian-Carboniferous and Permian-Mesozoic successions.

The NW-SE trending Koszalin Fault is regarded as the offshore prolongation of the eastern boundary of the Koszalin-Chojnice Structural Zone (KCSZ). Geological interpretation of the LT-7 deep refraction profile (Guterch et al., 1994) shows the Koszalin Fault as the distal antithetic break-off in the hanging wall (Berthelsen, 1998); other antithetic faults rotate the downfaulted

110 basement and pre-Permian cover southwest of the Koszalin Fault (Antonowicz et al., 1994). Offshore Poland, the Koszalin Fault delimits the boundary between the Darłowo and Kolobrzeg tectonic blocks and it is associated with deformations in the sub-Permian and Mesozoic strata. The strongly localised subsidence occurred mostly in the Triassic and Jurassic periods, presumably as a result of local strike-slip displacements, transtension, and the creation of small pull-apart basins (Pietsch and Krzywiec, 1996; Krzywiec, 2002). Later, due to NE-SW compression, this entire tectonic system was inverted during the Late

115 Cretaceous/Paleocene time (Antonowicz et al., 1994). The extensional fault system reactivated reversely in the pre-Zechstein basement is accompanied by asymmetric fault-propagation folds generated within the Mesozoic infill (Schlüter et al., 1997; Dadlez et al., 1995; Kramarska et al., 1999; Krzywiec, 2002).

3 Dataset used in the study and methods

3.1 Dataset used in the study

120 The BalTec 2D MCS data were acquired in March 2016 onboard R/V Maria S. Merian by the Federal Institute for Geosciences and Natural Resources Germany (BGR) (for details see Hübscher et al., 2017). The main acquisition parameters and an example of a raw shot gather are presented in Table 1 and Figure 2a respectively. Around 850 km of the BalTec data were recorded in the Polish sector. The location of the selected BalTec profiles is shown in Figure 1bB.

The PGI97 2D MCS data were acquired in 1996-1997 as a collaboration of the Polish Geological Survey (PGI) and the

125 Netherlands Institute of Applied Geophysics (TNO) (Kramarska et al., 1999; Krzywiec et al., 2003). This project aimed to image the geology of the upper 400 meters beneath the sea bottom to prepare a new geological map of the Baltic Sea (Kramarska et al., 1999). The dataset consists of several profiles extending to German, Danish and Swedish sectors, with a total length of 4000 km. The main acquisition parameters and an example of a raw shot gather are shown in Table 1 and Figure 2b respectively. Two profiles were selected to complement the BalTec data for interpretation purposes in this study. Available

130 pre-stack data (raw shot gathers) transcribed from original tapes by PGI make the reprocessing possible.

BalTec and PGI97 data were complemented by the DBE (Danish Bornholm Enclave) dataset, acquired offshore Bornholm in 1982 by Western Geophysical. Geological Survey of Denmark and Greenland (GEUS) provided us with the selected profiles (21 profiles in the Danish territorial water). Only post-stack time migrated versions were available.

In this study, in order to image the Koszalin Fault, CDF and the sedimentary cover overlying TTZ, 5 profiles were selected from 3 different datasets~~data vintages~~ (see Fig. 1 for locations): 2 profiles ~~of~~from the BalTec data (BGR16-258, BGR16-212), 2 profiles ~~of~~from the PGI97 data (PGI97-13, PGI97-202) and 1 profile ~~of~~from the DBE data (DBE-6A). The selected sections run from the vicinity of the Polish coast toward the Amager tectonic block in the Danish waters. Most of the seismic sections are oriented from the northeast to the southwest, and perpendicular to the Koszalin Fault. Unfortunately, well data information is very limited for this study. Only the SW end of profile BGR16-258 is calibrated by deep well L2-1/87 (Fig. 1b). The borehole information is limited offshore Pomerania because this area is considered less favourable for hydrocarbon exploration (Karnkowski et al., 2010). However, our seismic interpretation relies on publicly available data from all offshore wells shown in Figure 1 (G14-1/86 (Seidel et al. 2018), Pernille-1, Stina-1 (Vejbaek et al. 1994; Graversen, 2004), K9-1/86, K1-1/86, L2-1/87, A8-1/83 (Rempel, 1992; Schlüter et al., 1997; Krzywiec, 2002)).

Survey name		BalTec	PGI97
General	Recorded by	The Federal Institute for Geosciences and Natural Resources (BGR)	The Netherlands Institute of Applied Geophysics (TNO)
	Party/Vessel	RV Maria S. Merian	Dr. Lubecki
	Positioning system	DigiCOURSE System 3	DGPS System
	Date	March, 2016	September, 1996
Seismic source	Type	Airgun	Airgun
	No. guns	8	1
	Capacity	250 cu. in.	10 cu. in.
	Shot interval	25 m	12.5 m
	Source tow depth	3/6 m	1.5 m
Receivers	Number of channels	216	12
	Channels interval	12.5 m	12.5 m
	Cable tow depth	4 m	1.5 m
	Nearest offset	32.8 m	25 m
	Furthest offset	2724.2 m	162.5 m
	Record length	8500 ms	800 ms
Recording system	Sample rate	1 ms	0.5 ms

Table 1~~1~~: Acquisition parameters for the two seismic surveys: BalTec and PGI97.
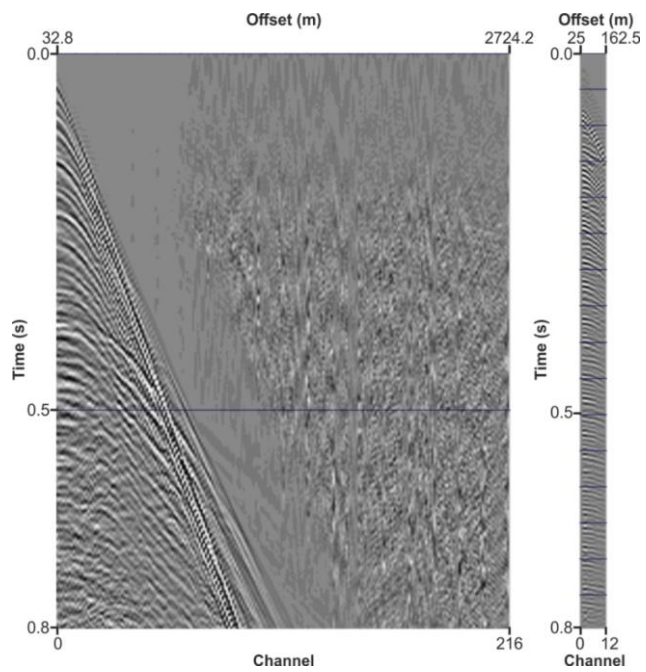
145
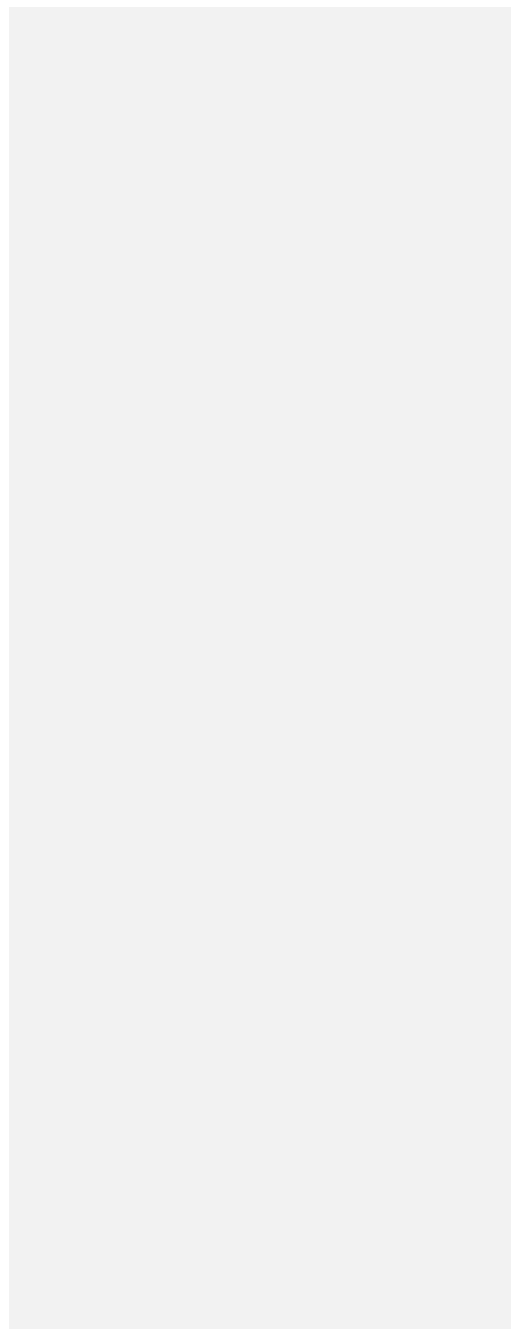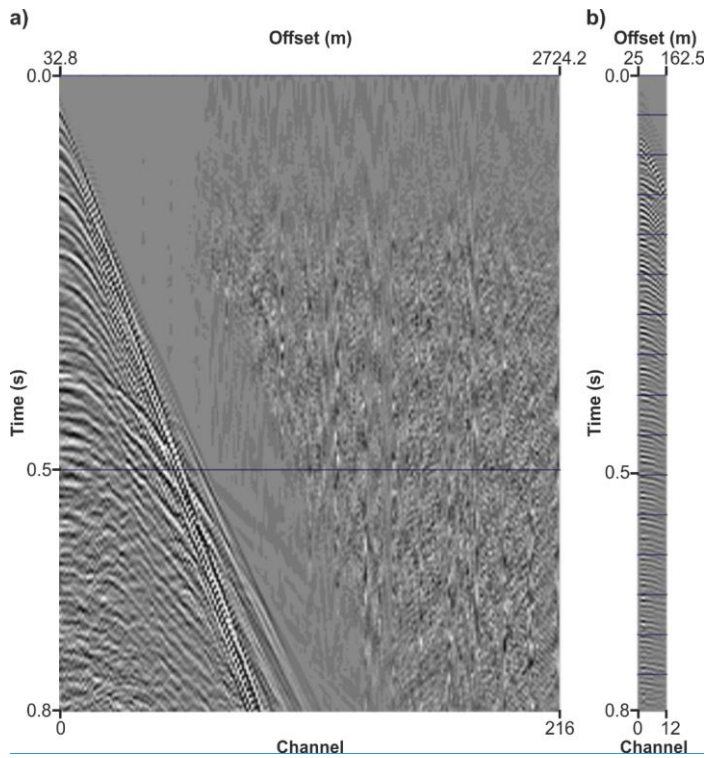
Figure 2: Raw shot gathers from the two different surveys (BalTec ~~(a)~~ and PGI97 ~~(b))~~. Notice the large difference in terms of the number of channels between the two datasets.

~~**3.2 Multiple reflection elimination strategies**~~

150 ~~Multiples reflection (multiples) are a constant problem for marine seismic data and an even more challenging issue in shallow waters. The water depth of the southern Baltic Sea is around 10 to 50 m. Therefore, the seismic records in this area will be always contaminated with multiple reflections, especially at near seafloor intervals. There are several ways to classify multiples (Fig. 3). Depending on where the ray path's downward reflection occurs, multiples can be categorized into surface-related multiples and internal multiples. Internal multiples have one downward bounce at the first reflector and no downward bounce~~
155 ~~at the surface. Surface-related multiples have two downward bounces at different reflectors: one at the surface and one at the first reflector (Verschuur, 2013). Multiples can be also classified as long-path and short-path based on their time delay from~~

the primary events (Sheriff and Geldart, 1995). Long-path multiples can be separated from the primary events as their travel path is much longer than the primaries, therefore, they appear at different arrival times in the seismic data. In contrast, short-path multiples are those that cannot be observed as separate events from the primaries that generate them (Verschuur, 2013).

160   The application of multiple reflection removal (demultiple) methods is dependent on the properties of the multiple presented in the seismic data (Verschuur, 2013). There are two main categories: (1) methods based on a difference in spatial behaviour of primaries and multiples; and (2) methods based on periodicity and predictability. The former is typically based on filtering methods such as τ-p deconvolution, Radon demultiple or stacking, which exploits the differences in velocities and/or reflecting structures between the primaries and multiples. The latter relies on the prediction from either modelling or inversion of the

165   recorded seismic wavefield (Weglein, 1999). Surface-related multiple elimination (SRME) or wavefield extrapolation methods are among this category (Verschuur, 2013). In our processing workflow, we included both categories of multiple elimination methods in order to handle different multiples existing in the 2D shallow marine seismic data.
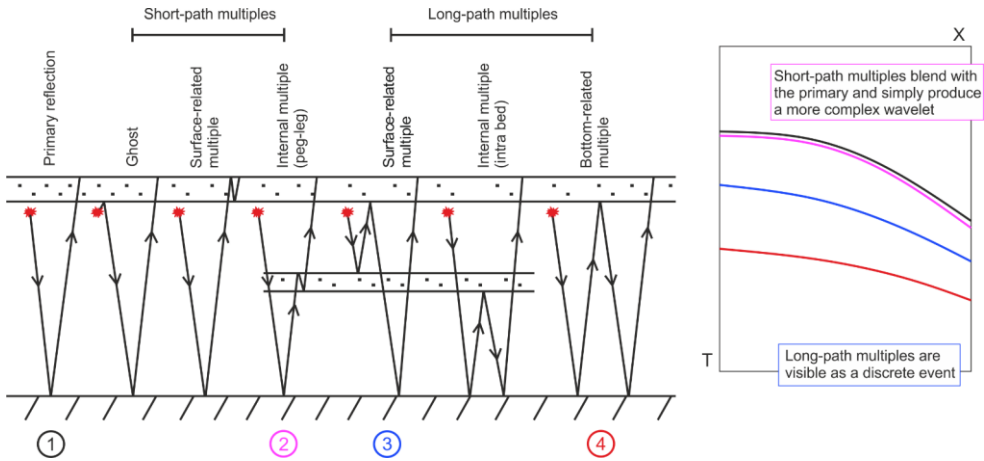
Figure 3: Basic types of multiple reflections (modified from Sheriff and Geldart, 1995).

170   **4 Processing of seismic data**

Here we provide basic description of the processing workflow applied to the new BalTec data, as well as reprocessing of the PGI97 data. More details are provided in the accompanying Supplementary Material including Supplementary Figures S1 to S5.

BalTec – workflow	

1	Read SEG-D data and assign geometry
2	Streamer and shot depth statics
3	Spherical Divergence Correction
4	Swell noise attenuation
5	SRME
6	Predictive deconvolution in the τ-p domain and τ-p mute
7	Data regularisation
8	Water bottom F-K filtering
9	Velocity analysis
10	High-resolution parabolic Radon demultiple
11	F-X deconvolution
12	Bandpass filter
13	Phase conversion
14	Pre-stack time migration
15	Front mute
16	AGC
17	Stacking
19	Post-stack processing (Trace mixing)

Table 2: Processing workflow applied to BalTec data.

175

BalTec workflow	
1	Read SEG-D data and assign geometry
2	Streamer and shot depth statics
3	Spherical Divergence
4	Swell noise attenuation
5	SRME
6	Predictive deconvolution in the τ-p domain and τ-p mute
7	Data regularisation
8	Water bottom F-K filtering
9	Velocity analysis
10	High-resolution parabolic Radon demultiple
11	F-X deconvolution

~~12~~	~~Bandpass filter~~
~~13~~	~~Phase conversion~~
~~14~~	~~Pre-stack time migration~~
~~15~~	~~Front mute~~
~~16~~	~~AGC~~
~~17~~	~~Stacking~~
~~19~~	~~Post-stack processing (Trace mixing)~~
PGI97 – original workflow	
1	Read SEG-Y data and assign geometry
2	Static shift (shot delay)
3	Amplitude recovery
4	Velocity analysis
5	NMO correction
6	Stacking
7	Post-stack predictive deconvolution
8	Bandpass filter
PGI97 – new workflow	
1	Read SEG-Y data and assign geometry
2	Static shift (shot delay)
3	Resample
4	Source signature deconvolution
5	Bandpass filter
6	Spherical Divergence Correction
7	Pre-stack predictive deconvolution
8	Water bottom F-K filtering
9	Velocity analysis
10	Bandpass filter
11	Front mute
12	AGC
13	Stacking
14	Post-stack time migration
15	Post-stack predictive deconvolution

16	Trace mixing

Table 32: RePprocessing workflow applied to BalTec and PGI97 data and the original processing workflow of PGI97 data.

4.1 Processing of the new BalTec data

Multiple reflections are the major problem faced when processing seismic data acquired in the Baltic Sea due to the relatively shallow water depth (average water depth around 50 m), and the new BalTec survey is not an exception. Therefore, removing multiples reflections (hereinafter referred to as demultiple) was central throughout the entire processing flow for these data. Based on analysis of the properties of multiples present in seismic data (both in the shot domain and the CDP domain), the demultiple workflow consisted of (i) Surface-Related Multiple Elimination (SRME) method, (ii) water bottom F-K filtering (periodicity and predictably based methods), (iii) predictive deconvolution in the τ-p domaindeconvolution, and (iv) high-resolution parabolic Radon demultiple (difference in spatial behaviour based methods) (Harlan et al. 1995). The order of demultiple applying these methods in the processing workflow is shown in Table 2 and discussed in more detail in the Supplementary Material. The effectiveness of our approach is illustrated in Supplementary Figure S1 and S2. The cascaded demultiple approach in the BalTec processing workflow improved the velocity analysis as well as helped to produce the final pre-stack time migrated (PSTM) stack sections optimal for subsequent seismic interpretation. Even though the structures in the area are only moderately dipping, we evaluated the PSTM approach as superior to the post-stack time migration used during onboard processing (Fig. 3). More details about the velocity analysis, together with the examples of the velocity models (Fig S4 and S5), as well as the details on PSTM are provided in the Supplementary Material. Seismic gathers in the shot and CDP domain after each demultiple method are compared in Figure 4. A series of stack sections after each demultiple approach are shown in Figure 5.

SRME is a method using a data-driven algorithm for removing multiples (Verschuur et al., 1992), it is often applied earlier than other demultiple approaches in the processing flow. However, SRME's efficiency is largely affected by the signal-to-noise ratio of the input data. Therefore, gun and cable static correction, spherical divergence, and other incoherent noise attenuation approaches should be applied to the SRME input while maintaining the amplitudes and phase of recorded primaries and multiples. The shot point interval is 25 m while the channel interval is 12.5 m. Therefore, to construct the multiple estimates, the shot points were interpolated to 12.5 m, and the record data is extrapolated to zero offsets. A mute is applied to the input shot records prior to removing direct arrival energy and the first seafloor multiple. After surface-related multiple is modelled by a series of convolutions and summation, the output model shot point is renumbered back to the same order as the original shot gathers for the subtracting process. For this data, a three-passes approach for SRME adaptive subtraction including two subtraction processors based on two publications by Wang (2003) and Monk (1993) is applied.

The τ-p predictive deconvolution method is applied following the SRME method. The main aim of τ-p deconvolution for this dataset is to remove short-path multiples. At the same time, muting performed in the τ-p domain attenuates linear noise and

seismic interference. The input data is transformed to the τ-p domain using linear transform (Stoffa et al., 1981; Zhou and Greenhalgh, 1994), Wiener deconvolution (design window of 240 ms of operator length and 48 ms of gap length) is applied to the whole traces. After τ-p deconvolution, in order to improve signal-to-noise ratio and enhance deeper imaging data were regularized in 2 steps. Firstly, the shot records are interpolated to 12.5 m of shot point interval from the nominal 25 m recorded, which doubled the CDP fold. Secondly, decimating the fold of the shot gathers from 216 to 113 to get to a 25 m receiver interval and 12.5 m CDP interval so the spatial sampling at 12.5 m is more beneficial to image the deeper part of the sections.

210
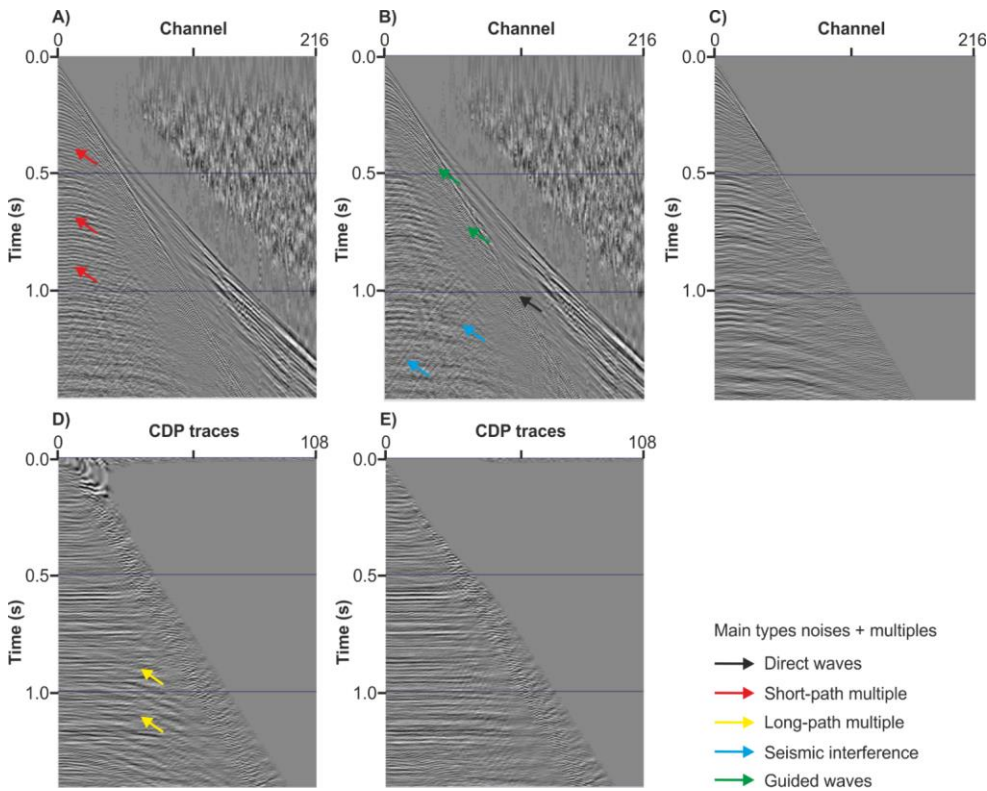
Figure 4: Example of shot gathers and CDP gathers after the main processing steps of the BalTec data. A) Raw shot gather; B) Shot gather after SRME; C) Shot gather after τ-p deconvolution; D) CDP gather after water bottom F-K filtering (input for

215 Radon demultiple); E) CDP gather after Radon demultiple. The main types of noises and multiples are highlighted by arrows. Notice how different events are attenuated after each demultiple approach.

Because of the very shallow water bottom, SRME does not successfully eliminate strong water bottom multiples. Therefore, to remove them, we used a simple technique in which the data are flattened according to the travel time of the water bottom multiple followed by a F-K reject mute to remove flattened multiple energy (see Nguyen, 2020). This procedure (called the 220 water bottom F-K filtering approach) can be repeated for the N-th water bottom multiple. Here we applied up to three passes.

Parabolic Radon demultiple (PRT demultiple) is applied to target the long-path multiples as SRME and τ-p predictive deconvolution methods are inefficient for these types of noises. The normal PRT demultiple has some limitations, so a Harlan signal extraction filter (based on Harlan, 1995) is used to overcome the limitations (this approach was called high-resolution PRT demultiple). This filter provides a high-resolution Radon transform by taking the PRT of the input data, and the muted 225 PRT of the input data with trace polarities randomly reversed and put these into Harlan's signal extraction algorithm to focus on the signal in the PRT domain. The high-resolution PRT demultiple is applied with a start time of 500 ms as artefacts are introduced in the near-surface, where move-out values are large and reflections only exist at near offsets. Optionally, this approach also is reapplied after each velocity analysis pass.

In order to enhance the signal, F-X deconvolution is applied to remove random noise in CDP gathers. F-X deconvolution is a 230 process designed to effectively attenuate random noise by prediction of the non-random signal content in a seismic trace. Each input trace is transformed into the frequency domain. Groups of traces are used to design filters to predict the Fourier components of adjacent traces. The filtered section is finally transformed back into T-X space, and the noise component is removed. NMO correction is applied before and removed after applying F-X deconvolution.

The velocity models were determined using the interactive velocity analysis program (Global Claritas CVA). Generally, 235 velocity analysis was carried out in 3 passes: the first pass velocity is picked before the high-resolution Radon demultiple, the second pass is picked and updated before pre-stack time migration, and the third pass is checked and updated the second pass velocity after migration. Velocity was picked at every 500 CDP point for the first pass, then 250 CDPs (around 3.0 km intervals) for the next two passes. A straight-ray 2D Kirchhoff pre-stack time migration (PSTM) is performed using first-pass velocities to enhance data imaging. The main input of the migration process is pre-stack seismic data with geometry applied 240 and RMS velocity field. The pre-stack migration process is applied again when each pass of the velocity field is updated. Before stacking, a post-NMO outer trace mute is applied to remove any coherent noise on the outer traces and to reduce the effect of NMO stretching on the far offsets. To balance seismic amplitude across the section, a normal 500 ms window AGC scaling process is applied before and after stacking. The traces within each CDP gather were summed. The maximum number of traces in migrated CDP gathers is 108.

245   ~~More details of the BalTec data processing flow can be found in the BalTec seismic data processing report (see Nguyen, 2020).~~
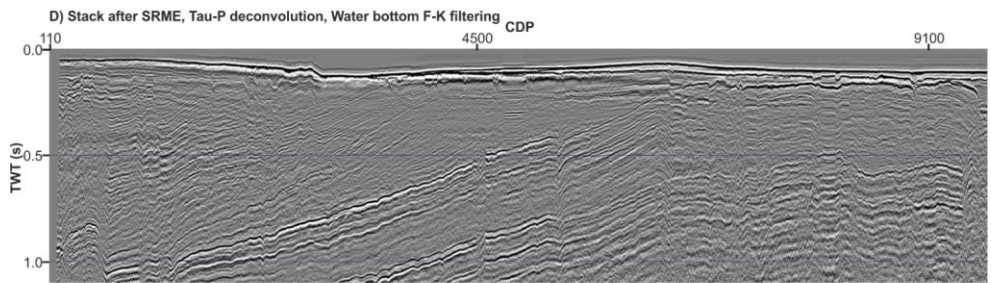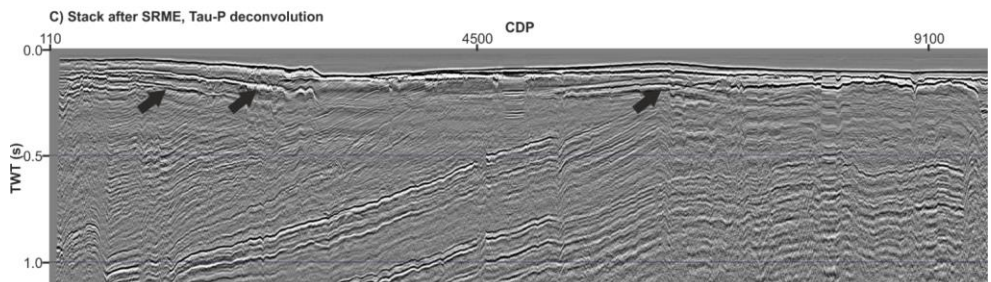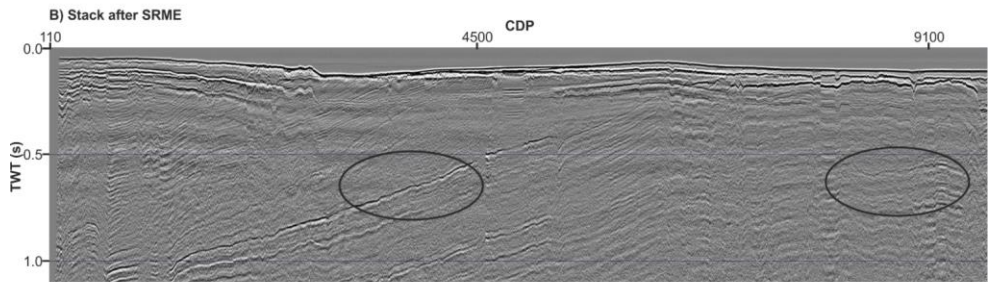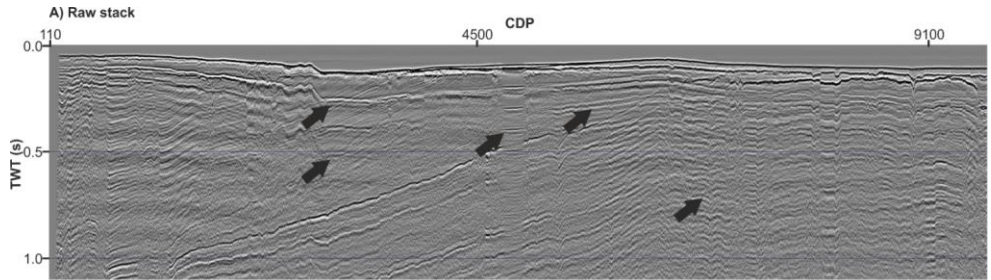
A) Raw stack

CDP

110   4500   9100

TWT (s)

B) Stack after SRME

CDP

110   4500   9100

TWT (s)

C) Stack after SRME, Tau-P deconvolution

CDP

110   4500   9100

TWT (s)

D) Stack after SRME, Tau-P deconvolution, Water bottom F-K filtering

CDP

110   4500   9100

TWT (s)

0 3 6 9
Distance (km)
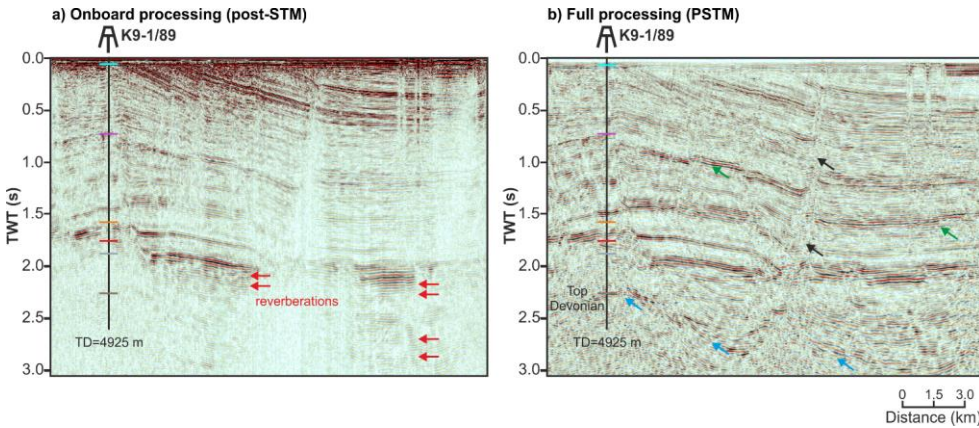
Figure 3: Comparison of BalTec onboard processing result (a) (Hübscher et al., 2017) and BalTec full processing result (b). Post-stack time migration and pre-stack time migration were applied in the onboard processing and in the full processing respectively. Notice the difference in the amplitude balance between 2 versions due to amplitude correction was not applied on the onboard processing. Particular image enhancements are highlighted by arrows.

4.2 Reprocessing of the vintage PGI97 dataset

The PGI 97 data were ~~initially~~ processed at TNO shortly after the survey (see the original processing flow in Table 3.~~, the processing flow can be found in Table 2. The original workflow includes a limited number of processing steps. Apparently, t~~The original processing was~~flow is~~ limited in~~to~~ demultiple approaches, especially before stacking, due to the limited ~~constraints on~~ demultiple techniques available at that time and the limitations of the data (short offsets).

An example of stacked sections created using the original workflow is shown in Figure 4a~~7A~~. Reverberations from the primary events are dominant across the seismic section. ~~Because of data acquired in a very shallow water environment, the first and second order of water bottom multiples are clear and conflict with the primary reflection on the shallow part of the section.~~ Additionally, the existence of high-frequency noise can be easily seen in the section, which can lead to the misinterpretation of the main geological features. ~~Secondly, the current~~ Previously, sections were stacked using a simple~~poor~~ velocity model and~~, which was represented by the poor image of the water bottom and shallow reflections, also primary events were not continuously imaged. Lastly, there was~~ no migration process was applied ~~in the original flow, the dipping events are mis-~~

positioned laterally and appear less steep than they really are, and diffractions events would interfere with primaries. Re-processing (see the workflow in Table 3) addressed all the above issues.

270 Re-processing workflow for the PGI97 data can be found in Table 2. Since the PGI97 data has a very short offset (150 m)only 12 channels) (Fig. 2b), the move-out-based (Radon demultiple) or model-based demultiple approaches (SRME) were not applied to this data. Only the predictive deconvolution approach was attemptedapplied before and after stacking. It efficiently attenuates severe reverberations and water bottom multiples (Fig. S36) and helps in velocity analysis. Apart from predictive deconvolution, the water bottom F-K filtering technique was also applied to this data to remove more multiples from the seafloor.

275 The velocity analysis from the original processing flow did not give the accurate interval velocities due to the length of the streamer (150 m total active length); therefore, re-picking of velocities was also carried out. Although the velocity analysis was limited by the available offset, there were still uncertainties on velocities due to the limit of traces in the CDPs gathers, the new velocity models were considered relatively good because they were picked on cleaner gathers robust enough and followingcomforming to the geological structure geology in the study area to produce improved stack sections. The data were 280 then migrated by a post-stack finite different time migration routine (Claerbout and Doherty, 1972) using the new smoothed velocity model (Figure 74c).
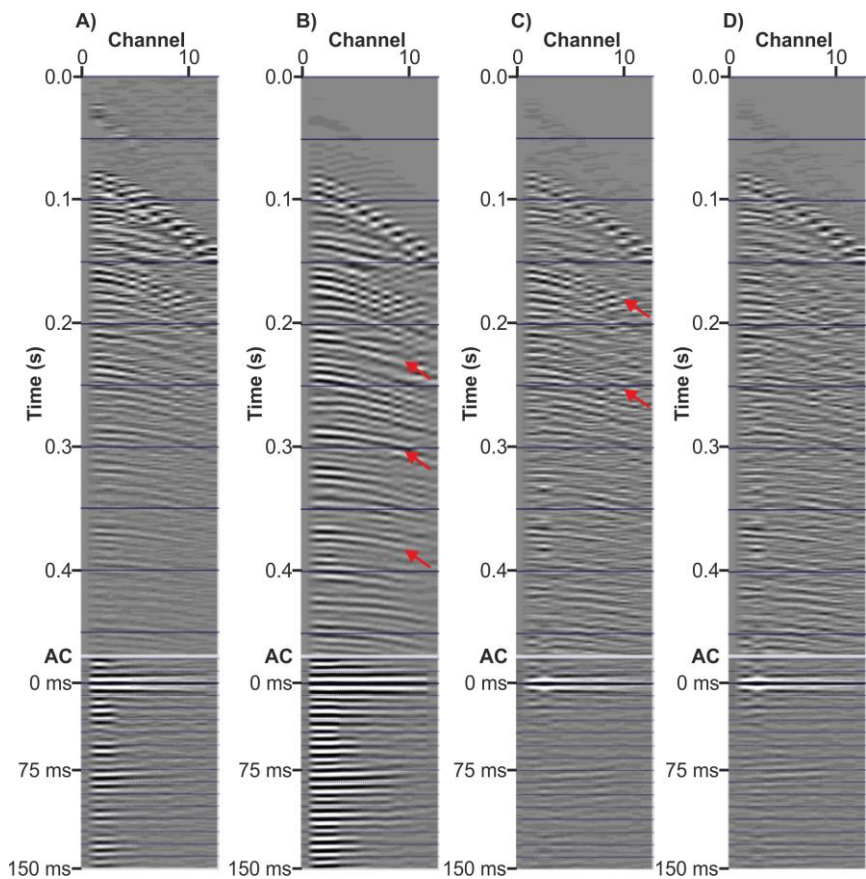
Figure 6: Example of shot gathers after main processing steps of the PGI 97 data and their autocorrelation (AC); (A) Raw shot gathers, (B) Shot gathers after FK mute and spherical divergence, (C) Shot gathers after predictive deconvolution, (D) Shot gathers after water bottom F-K filtering. Notice the visible attenuation of reverberation in the AC after the predictive deconvolution.
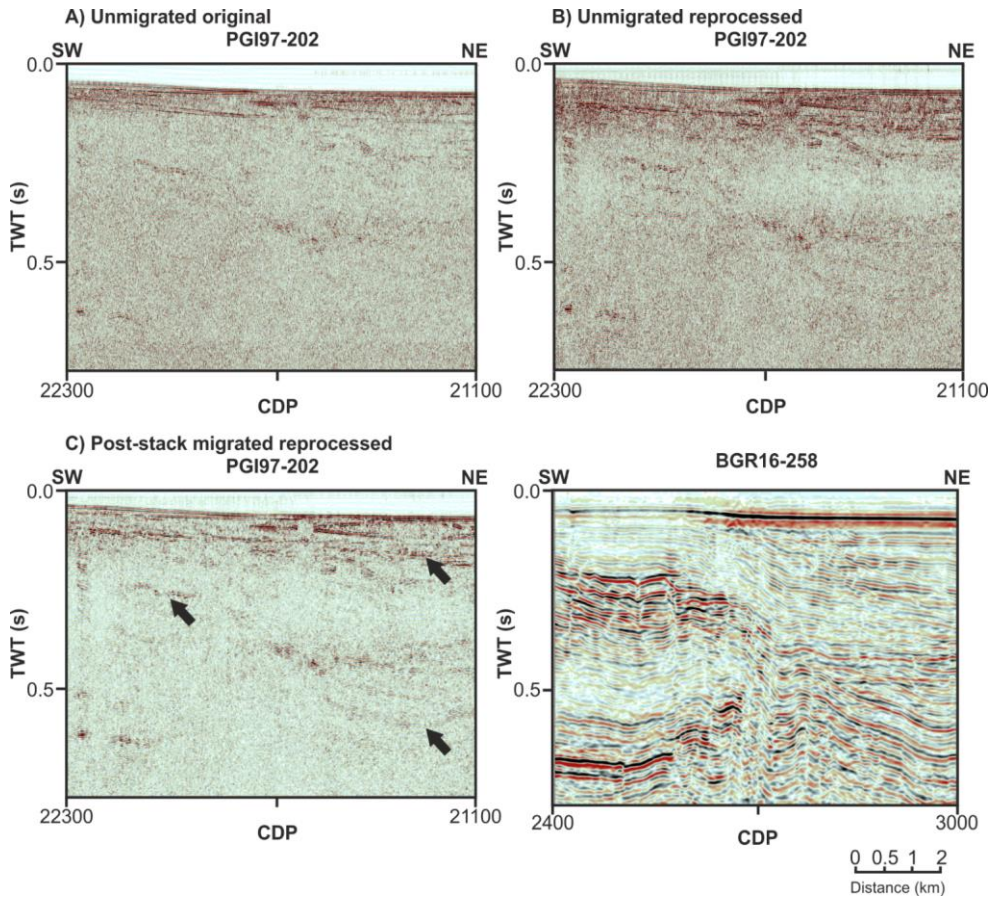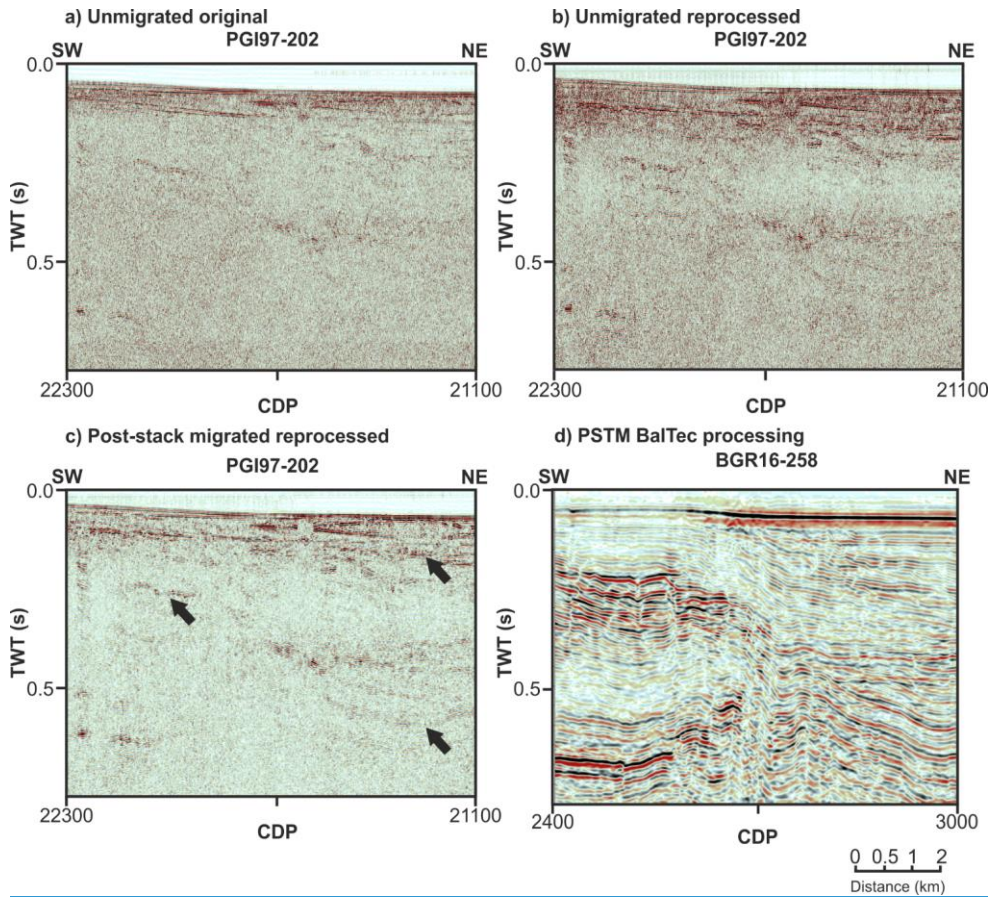
Figure 47: Comparison of part of final stack sections of vintage PGI97-202 profile: unmigrated original (aA), unmigrated reprocessed (bB), and migrated reprocessed (cC) with the parallel new BGR16-258 profile (d) at nearby location (see Fig. 1). Black arrows show the noticeable enhancement between the original processing flow with reprocessing flow.

5 Results

Compared to the onboard processing results (Hübscher et al., 2017) (Fig. 3a), the new processing of BalTec data (Fig. 3b) significantly enhanced reflection events (green arrows in Fig. 3b), fault planes (black arrows in Fig. 3b), and more importantly deep reflection events (ex. The top Devonian represented by blue arrows in Fig. 3b). Short-path multiple (red arrows in Fig. 3a) was also suppressed in the full processing version. It is due to the interplay of multiple elimination, improved velocity analysis, and pre-stack time migration (as opposed to post-stack migration used during onboard processing).

The processing of the PGI97 data bring significant improvement in the signal-to-noise ratio, especially in the final migrated stacked image (Figure 4c). Since the overall continuity of reflection events is improved, fault displacements are much easier to interpret. Dipping events are imaged at their true locations after migration. However, despite a lot of effort in reprocessing workflow to suppress multiples, the remnants of multiples still exist in the data. The parallel profile BGR16-258 (Figure 4d) provides a much better image of the shallow sediments overlying the Koszalin Fault compared to the profile PGI97-202. This proves the remarkably better quality of the newly acquired long-offset data over the legacy short-offset profiles.

Differences in term of both vertical and horizontal resolution between the BalTec and PGI97 high resolution data are highly noticeable. It is due to acquisition parameters and configurations, and purpose of the two datasets. In the final processing results, as focusing on investigation of the shallow sediment (up to 400 ms TWT), the PGI97 data frequency bandwidth and CDPs distance was limited between 100-400 Hz and 6.25 m respectively. Whereas the BalTec data frequency bandwidth and CDPs distance was limited between 8-80 Hz and 12.5 m respectively because the BalTec data aim to image deep Paleozoic stratigraphy events. The higher resolution and quality of the BalTec data allows the easier to interpret the Koszalin Fault zone especially in the shallow part (Fig 4c and 4d).

The final PSTM sections of BalTec data demonstrate reflection patterns of each sedimentary formation (Fig 5), these reflection patterns also represent for general lithology information from previous studies. In the EEC, the Precambrian crystalline basement is represented by chaotic pattern with low to medium amplitude, the basement is overlaid by thin Ordovician-Cambrian formation (~0.2 s TWT) is represented by semi- to high continuous parallel pattern with medium to very high amplitude. On top of the Ordo-Cambrian formation, a thick Silurian succession (from 1.0 to 1.5 s TWT) displayed by chaotic and continuous parallel reflection with low to high amplitude is deposited. In the WEP, the boreholes penetrate solely down to Devonian formation, therefore, in this study all below sedimentary successions are called pre-Carboniferous formation. The pre-Carboniferous formation is displayed of mixture of chaotic and discontinuous reflection pattern with low to medium amplitude, while the Carboniferous formation (thickness ~0.5 s TWT) represented by inclined parallel reflection pattern. The Permian formation is composed of very high amplitude local very thin Rotliegend deposits overlaid by medium to high

amplitude Zechstein. Reflection patterns of the thick Mesozoic deposits (~1 to 2 s TWT) are relatively consistent by semi- to
325   high continuous parallel events with low to high amplitude.

Formatted: Font: 10 pt
Formatted: Font: 10 pt
Formatted: Font: 10 pt
Formatted: Font: 10 pt
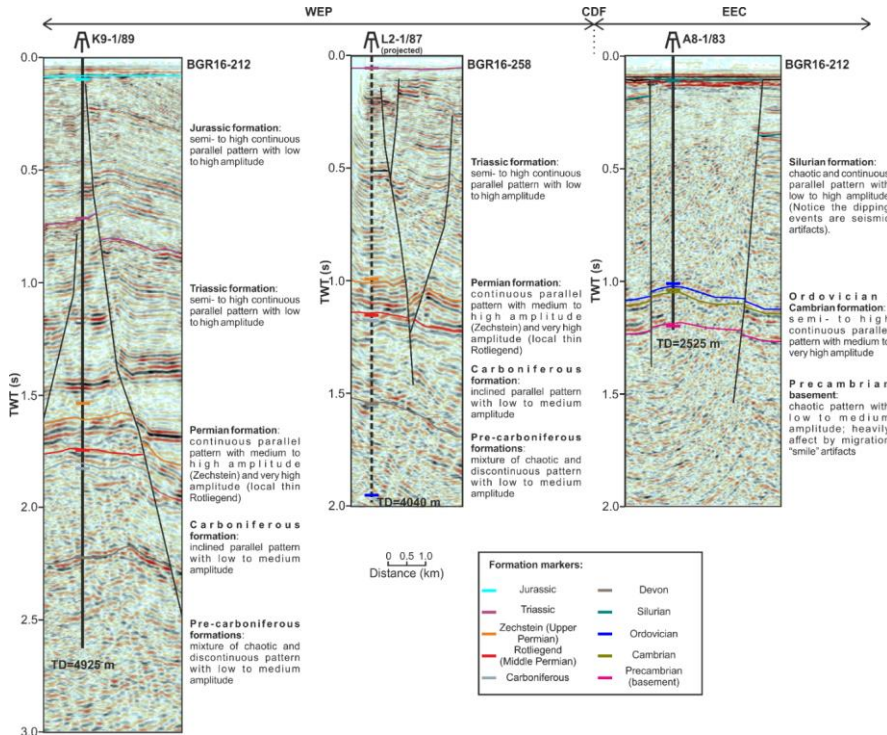
Figure 5: Well data to support interpretation (see Fig. 1b for locations) with the description of reflection patterns characteristics
for different stratigraphy units.

65 Seismic interpretation

330   Seismic interpretation is ~~demonstrated~~ presented for ~~the~~ selected 5 profiles (BGR16-212, BGR16-258, DBE-6A, PGI97-202,
and PGI97-13; Figs. 6-10~~8-11~~). As mentioned before, there is very sparse well control in the study area. For this reason, the
interpretation of these five profiles was carried out~~made~~ together with all other ~~the~~ profiles shown in Figure 1b~~B~~, and all
seismic profiles were tied to available well data ~~which in turn, were tied to all boreholes~~ in the study area. The seismic fabrics,
reflecting the structural features of the sedimentary cover at the locations of three of these wells, are shown in Figure 5. In the

seismic sections, the horizons are interpreted as the base of each formation. It is worth noting that previous research was taken into account in the research process in the south-western part of the Baltic Sea close to the Koszalin Fault~~The horizon interpretation was then extended to other profiles shown in Figures. 8-11 through cross sections. Southwest of the CDF, horizon identification mainly follows well L2/1-87 stratigraphy markers intersected by line BGR16-258 (Fig. 1B). Previous studies in the south-west of the Baltic Sea close to the Koszalin Fault were also taken into account~~ (e.g., Vejbaek et al., 1994; Krzywiec et al., 2003; Graversen, 2004; Pokorski, 2010; Jaworowski et al., 2010). ~~In the seismic sections, the horizons are interpreted as the base of each formation.~~

Profile BGR16-212

The section of the BGR16-212 profile used in this study crosses the CDF and the Koszalin Fault (Fig. 1~~8~~). The latter appears as a major inversion feature causing uplift~~ing~~ of Jurassic strata ~~on~~to the seafloor surface SW of the fault (Fig. 6). The uplifted Jurassic forms a core of the major inversion-related fold, the Kołobrzeg Anticline (Fig. 1b~~B~~). The anticline represents the offshore continuation of the Mid-Polish Anticlinorium that splits into the Kołobrzeg and Kamień Anticlines NW of the Polish coast (Fig. 1b~~B~~). The lack of Cretaceous strata suggests deep syn-inversion erosion. The amount of uplift cannot be estimated since the original thickness of the Jurassic and Cretaceous remains unknown. However, the minimum amount of uplift is constrained to 0.7 s TWT (~1 km) by the top of the pre-Carboniferous and top of the Jurassic. The presence of extensive Triassic and Jurassic strata as well as thin Zechstein and Carboniferous layers on the hanging wall of the reversed Koszalin Fault indicates that the latter was originally formed as a normal dip-slip fault (Fig. 6~~8~~). The minimum downthrown of the hanging wall can be estimated to 1.3 s TWT (~1.7 km), but this amount is only a minimum measure as missing part of Jurassic and entire Cretaceous is not included. Furthermore, the amount of pre-Zechstein erosion remains unconstrained.

The foot wall of the Koszalin Fault is onlapped by a Late Cretaceous syn-inversion marginal trough (Fig. 8a~~8~~). Seismic events within the foot wall show that the thickness change occurs away from the Koszalin Fault indicating syn-kinematic deposition during Late Cretaceous inversion (Fig. 8a). The trough fringes the uplifted core of the Kołobrzeg Anticline, attaining a thickness of 0.7 s TWT i.e., ~1 km. The rim of the Late Cretaceous trough onlaps the Koszalin Fault and the margin of the Kołobrzeg Anticline (Fig. 6~~8~~). Cretaceous sediments in the footwall are deposited directly on the Silurian substratum. This implies that the footwall was uplifted and eroded throughout the late Palaeozoic and Mesozoic until the late Cretaceous. The exact timing of uplift and erosion cannot be determined from the profile and this issue is addressed in the discussion.

The CDF coincides with the overthrust of the thrust-folded lower Palaeozoic on the mostly undeformed lower Palaeozoic strata of the Baltic Basin. The thrust has not been reactivated during the Late Cretaceous inversion. The amplitude of the overthrust as well as the timing of deformation cannot be inferred from seismic data. Nevertheless, the stratigraphic record (Podhalańska and Modlinski, 2010) points to the Silurian-Devonian transition as the time of folding and thrusting. The Caledonian thrust is of a thin-skinned character (Mazur et al., 2016), which is a feature~~characteristic~~ that is not entirely~~fully~~ clear from profile

BGR16-212. In the profile, the CDF coincides with the basement slope forming a frontal ramp of the thrust system (Fig. 68).
SW of the CDF, the top of the basement is located below the extent of the seismic data.
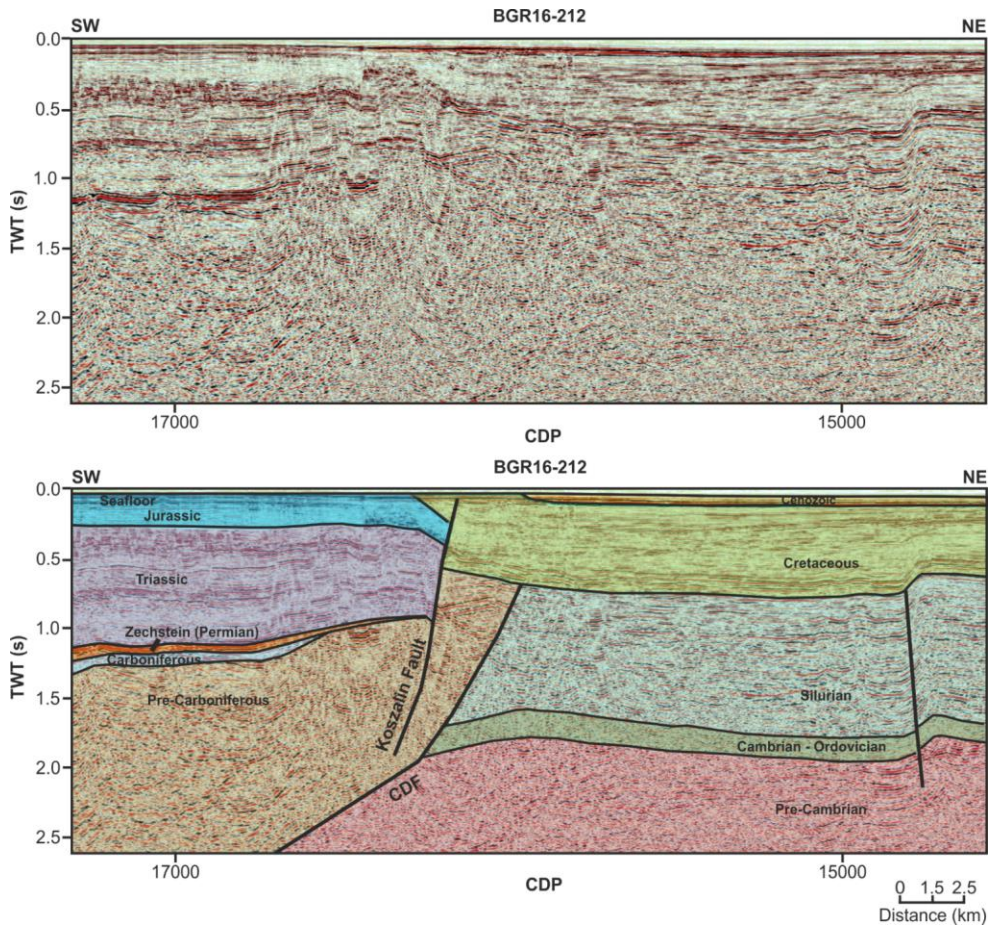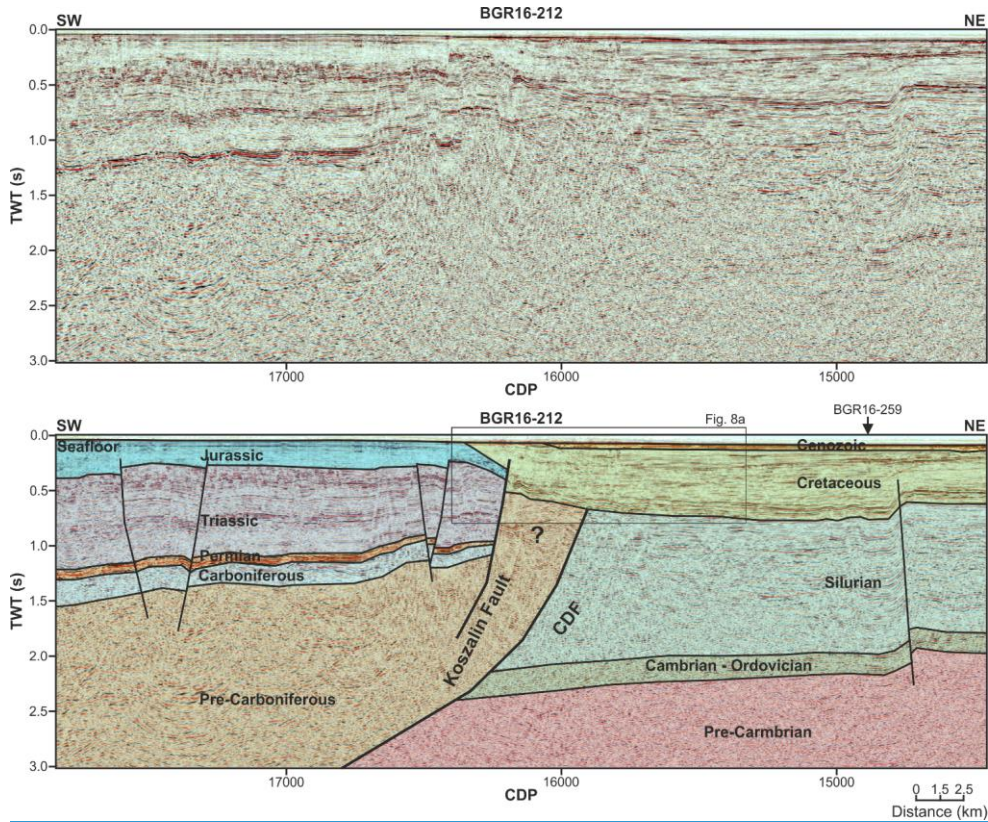
    Figure 68: Uninterpreted and interpreted part of BalTec line BGR16-212 (see Fig. 1 for location).

Profile BGR16-258

There are a numberseveral of similarities between profiles BGR16-258 and BGR16-212 (Figs. 68, 79). The Koszalin Fault
again appears as a major inversion feature uplifting Jurassic strata to the seafloor surface SW of the fault. At the extreme SW
of the profile, the Triassic is exposed at the sea bottom (Fig. 79). The uplifted Triassic and Jurassic form a core of the major
inversion-related Kołobrzeg Anticline (Fig. 1bB). The lack of Cretaceous and, in the far SW, also Jurassic strata suggests deep
syn-inversion erosion. Only a minimum amount of uplift can be estimated since the original thickness of the Jurassic and
Cretaceous remains unknown. Minimum uplift is constrained to 1 s TWT (~1.3 km) by the top of pre-Carboniferous and top

of Jurassic. The presence of extensive Triassic and Jurassic strata as well as Zechstein, Carboniferous and Devonian layers on the hanging wall indicates that the Koszalin Fault was originally formed as a normal dip-slip fault (Fig. 79). The minimum

380   downthrown of the hanging wall can be estimated to 1.3 s TWT (~1.7 km), but this is a minimum amount as missing Jurassic and Cretaceous is not considered. Moreover, two more faults, similar to the Koszalin Fault, occur farther SW. They cause another downthrow of the top of Silurian by 0.5-1 s TWT. The more southwestern of these two faults is a growth fault indicating Devonian syn-sedimentary extensional tectonics.

A Late Cretaceous syn-inversion marginal trough occupies the footwall of the Koszalin Fault (Fig. 79). The trough developed

385   next to the uplifted Kołobrzeg Anticline, attaining a maximum thickness of 0.8 s TWT i.e., ~1.1 km. The set of growth layers in the Late Cretaceous trough is consistent with syn-inversion sedimentation (Fig. 8b). The margin of the Late Cretaceous trough onlaps the Koszalin Fault and the adjacent part of the Kołobrzeg Anticline (Fig. 79), suggesting a continuation of erosion and subsidence sometime after the cessation of inversion. Cretaceous sediments cover a regional top Silurian unconformity proving deep pre-inversion erosion of the present-day foot wall of the Koszalin Fault.

390   The CDF coincides with the overthrust of the deformed lower Palaeozoic of the Pomeranian Caledonides on the tectonically undisturbed lower Palaeozoic of the Baltic Basin. As in line BGR16-212, there are no indications of the inversion-related reactivation of the Caledonian thrust. The latter is imaged as a relatively sharp boundary separating the orogenic wedge from the undeformed foreland. A nearby analogue of such a structure is the Carpathian Thrust Front in SE Poland, where a relatively sharp frontal thrust separates deformed sediments of the Carpathian foredeep from their undeformed equivalents (Krzywiec,

395   2001; Gągała et al., 2012; Krzywiec et al., 2014). The Caledonian thrust branches off from the top of the basement (Fig. 79) the slope of which forms a frontal ramp for the Caledonian fold-and-thrust belt (Mazur et al., 2016). The top of the basement slopes SW-ward below the extent of the seismic data.
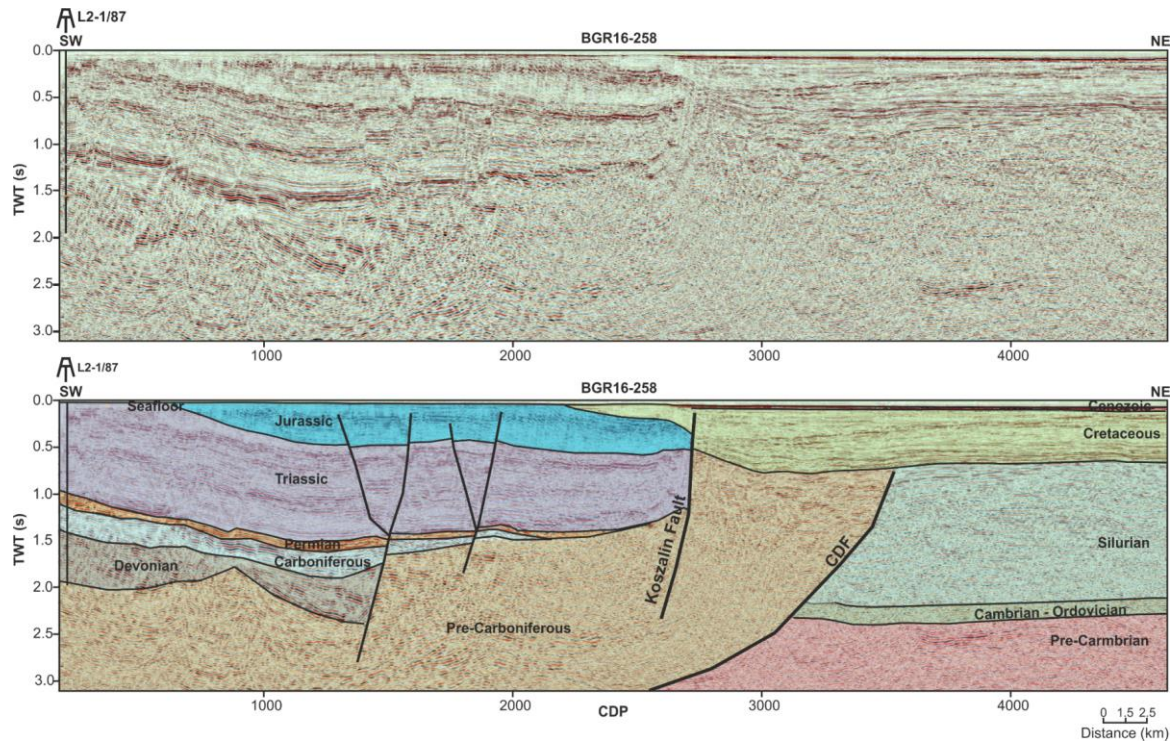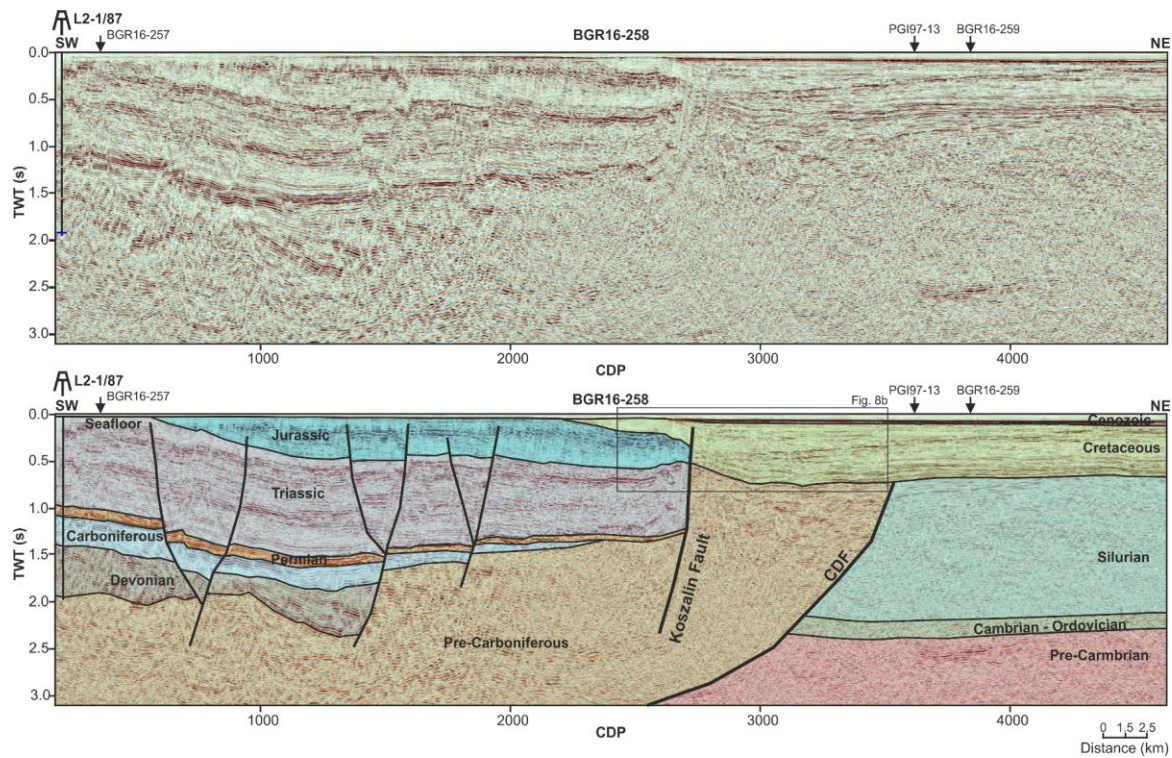
Figure 79: Uninterpreted and interpreted BalTec line BGR16-258 (see Fig. 1 for location).
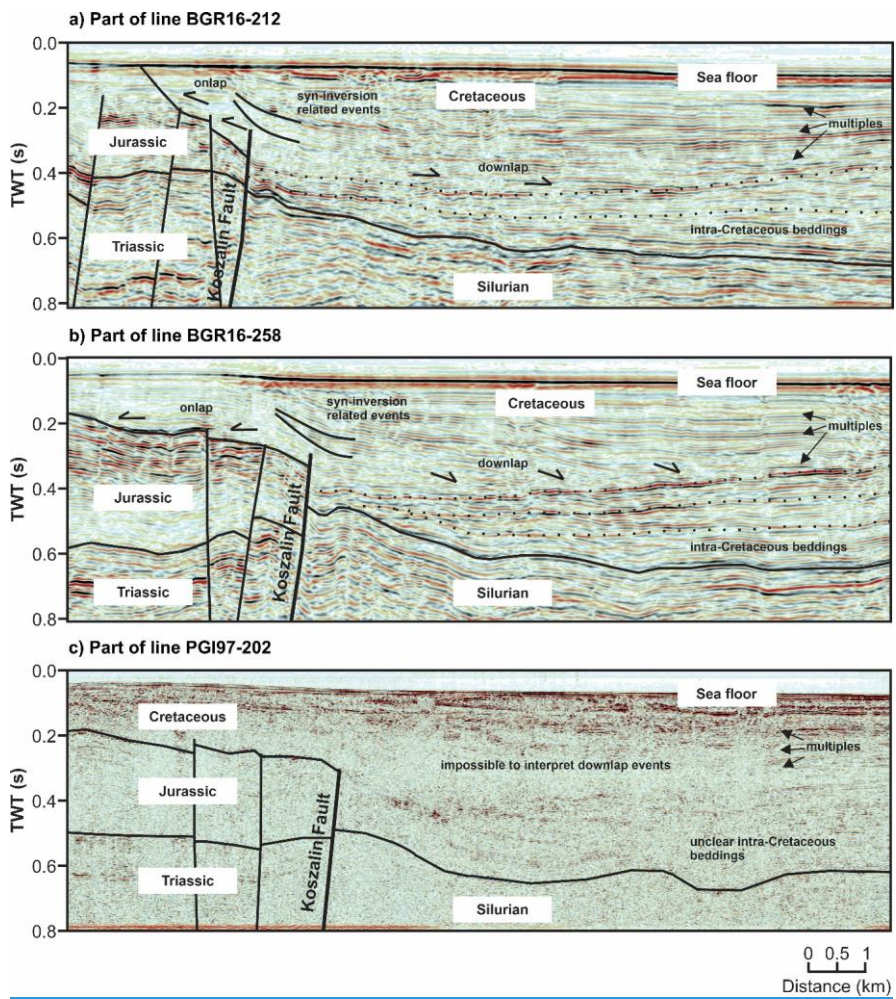
Figure 8: Zoom in part of seismic sections line BGR16-212 (a) and BGR16-258 (b) demonstrate geometry of reflections within the Cretaceous formation that related to the inversion movements of the Koszalin Fault. Similar geometry of reflections cannot be interpreted in the legacy PGI97-202 line (c) due to much lower quality data.

Formatted: Font: 10 pt
Formatted: Font: 10 pt
Formatted: Font: 10 pt

Profile DBE-6A

This is the NW-most profile out of the five presented in this paper (Fig. 1b~~B~~). In the DBE-6A line, the CDF is not imaged since it is located farther west beyond the termination of the seismic profile. This is the case since the CDF diverges away from the Koszalin Fault turning toward the WNW (Fig. 1b~~B~~). The Koszalin Fault is imaged again as an important inversion structure (Fig. 9~~10~~). Although in a map-scale picture the fault still represents the NE limit of the Kołobrzeg Anticline the seismic profile reveals a lower order fault-propagation fold within the hanging wall of the Koszalin Fault (Fig. 9~~10~~). The top of basement is also involved in folding that proves a thick-skinned character of deformation. The top of the basement is only slightly displaced and there is virtually no displacement for the top of Silurian. However, higher up, the Devonian to Jurassic strata are juxtaposed across the fault with the Upper Cretaceous fill of the marginal trough. It means that the original normal, down-dip displacement in the order of 0.7 s TWT (~0.9 km) was entirely reversed during the inversion phase. A foot wall of the Koszalin Fault is onlapped by the Late Cretaceous marginal trough that is c. 0.7 s TWT thick (~0.9 km).

Although profile DBE-6A lacks evidence for the end of Silurian and Caledonian deformation, it still documents the late Palaeozoic-Mesozoic subsidence in the hanging wall of the Koszalin Fault. This is demonstrated by the presence of the Carboniferous, Zechstein, Triassic, and Jurassic layers. This structural geometry indicates that the Koszalin Fault was originally formed in the late Palaeozoic as a normal, dip-slip feature. Furthermore, the seismic profile indicates that the structural domain characterised by late Palaeozoic or Mesozoic, pre-Late Cretaceous uplift and erosion is limited from the W by the Koszalin Fault and the CDF did not contribute to the development of the top Silurian unconformity in the area farther east.

An interesting feature represents another fault imaged near the NE termination of the profile (Fig. 9~~10~~). The fault cuts through the Darłowo Block (Fig. 1b~~B~~) from the top of the basement upward into the Late Cretaceous trough. This is clearly an inversion-related structure since it disturbs most of the Cretaceous succession (Fig. 9~~10~~). It also causes localised uplift of the top of the Cretaceous. The unnamed fault in question is a thick-skinned feature displacing the top of the basement by 0.25 s TWT (~0.7 km). Furthermore, the side branches jointly form a positive flower structure indicating a transpressional component during the Late Cretaceous inversion.

Profile PGI97-13 and PGI97-202

Profile PGI97-202 is parallel to the BGR16-258 line, running close to the north of it. In contrast, the PGI97-13 profile adjoins the BGR16-258 line at a high angle, being also oblique to the Koszalin Fault (Fig. 1b~~B~~). Both PGI97 lines image the Koszalin Fault quite schematically (Fig. 10~~11~~). The fault appears as an inversion structure with a reverse displacement in order of 0.2 s TWT. Both the profiles also document the previous dip-slip kinematics of the Koszalin Fault revealed by the increased thickness of the Jurassic strata in the hanging wall (Fig. 10~~11~~). As in the previously described profiles, the footwall of the Koszalin Fault is onlapped by the Late Cretaceous syn-inversion marginal trough. The PGI97 profiles image its thickness in

the range of 0.7 s TWT. Similar to the remaining seismic lines presented, the marginal trough onlaps the Koszalin Fault (Fig. 11) providing evidence for erosion and subsidence, continuing for some time after the termination of inversion. A characteristic feature, especially of profile PGI97-202, is the roughness of the top of the Cretaceous horizon (Fig. 1011), suggesting final

440   post-inversion uplift and erosion before the commencement of Cenozoic sedimentation.
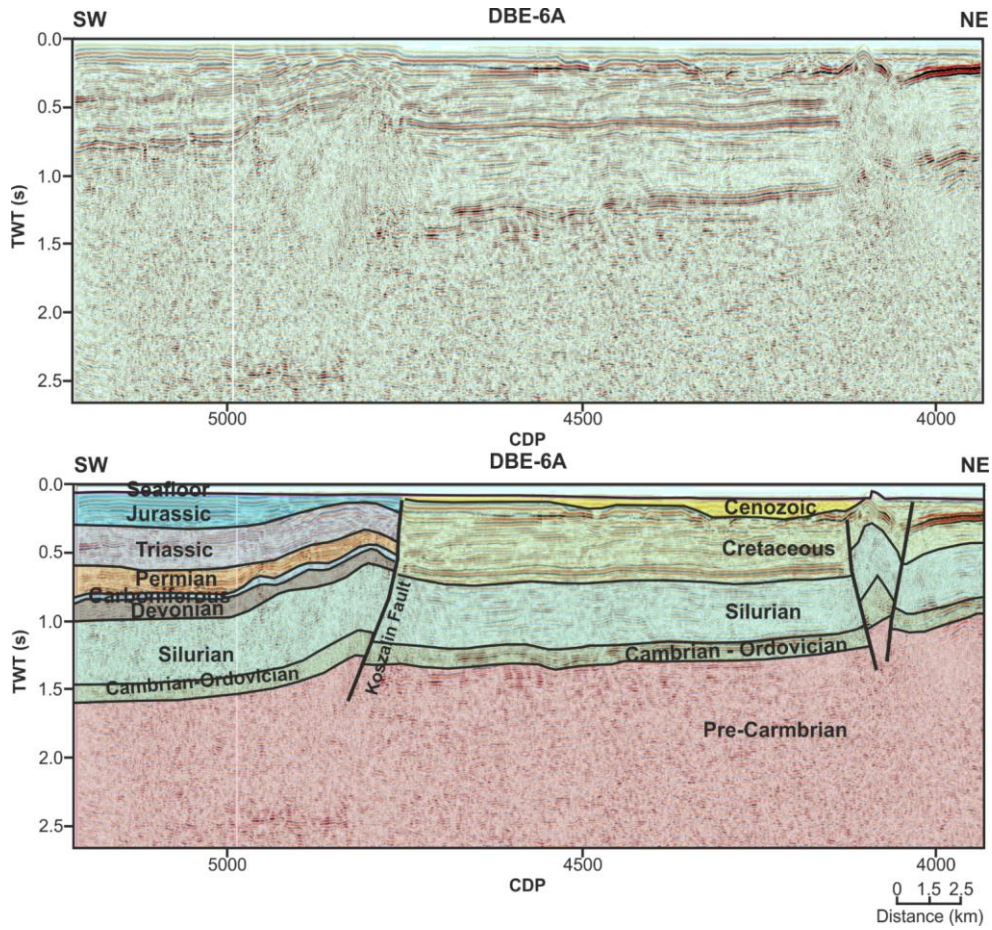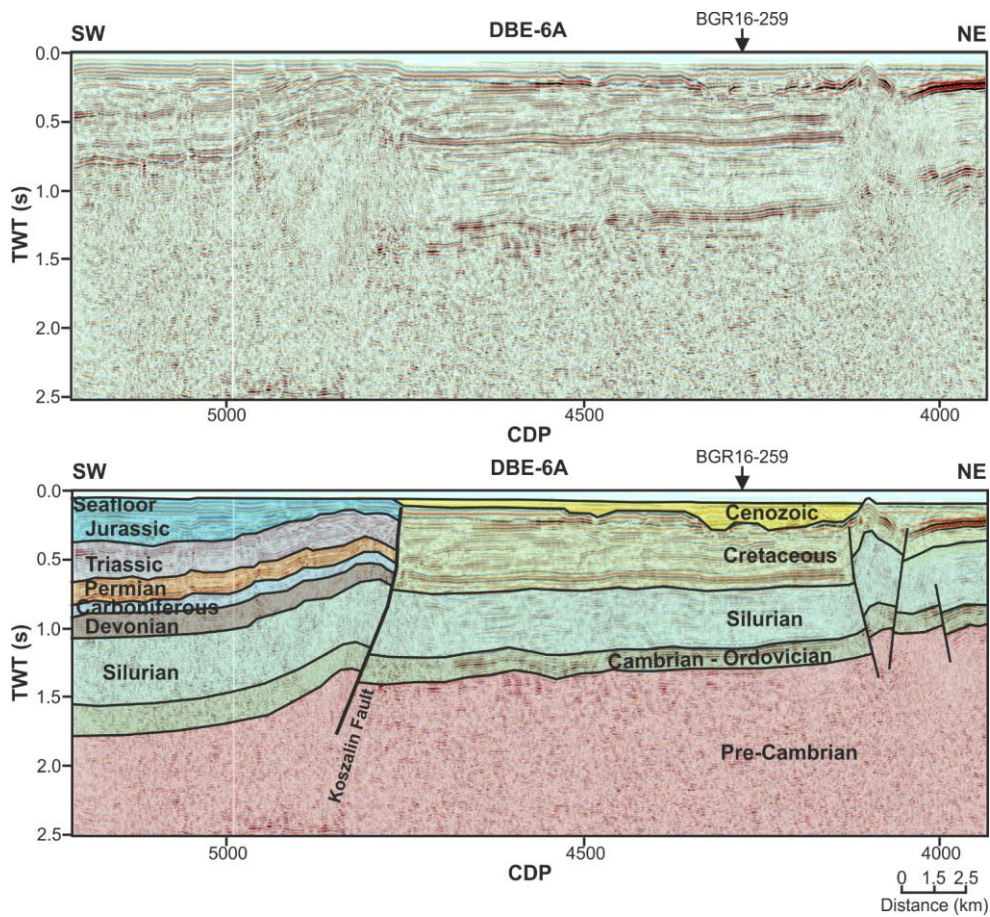
Figure 9~~10~~: Uninterpreted and interpreted GEUS seismic line DBE-6A (see Fig. 1 for location).

445
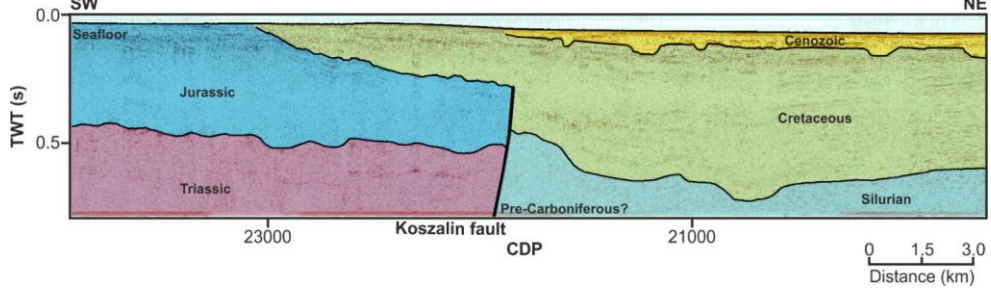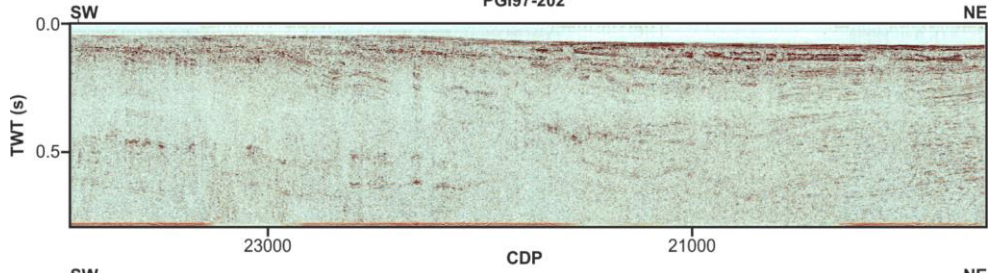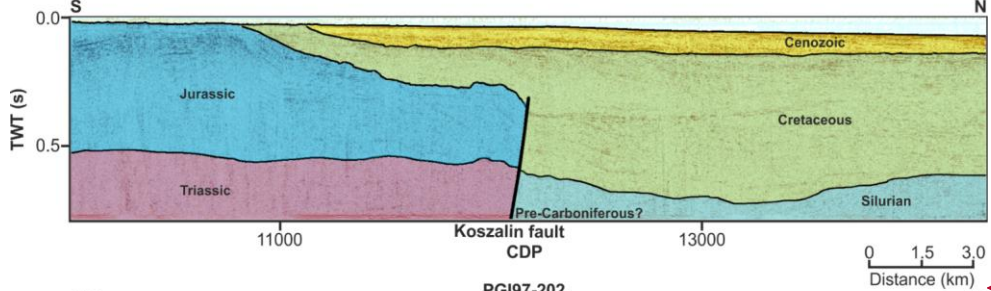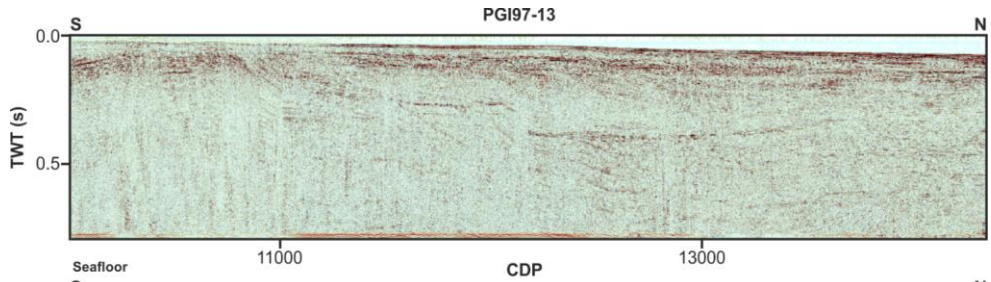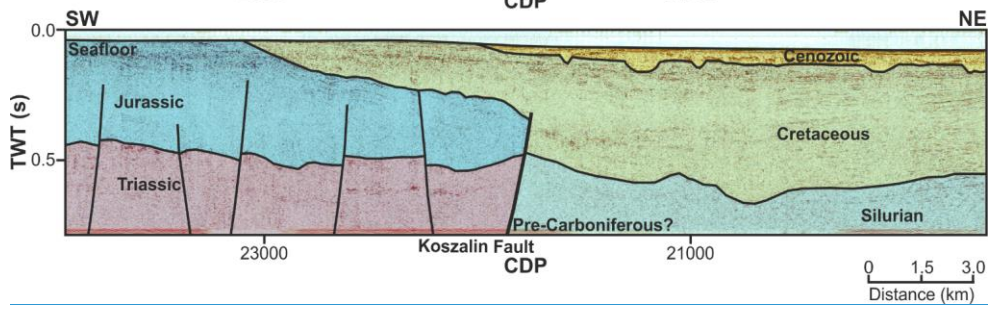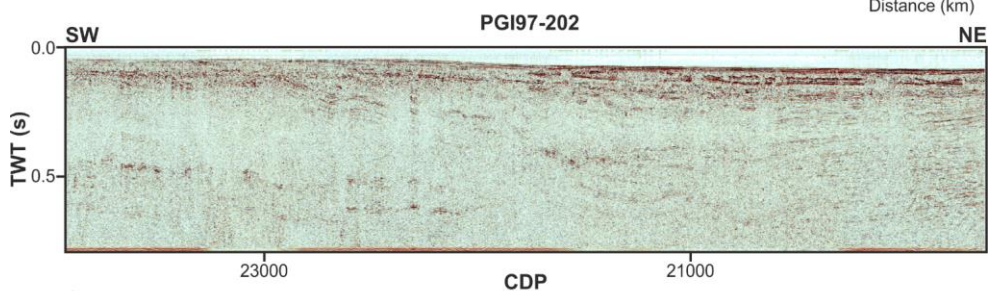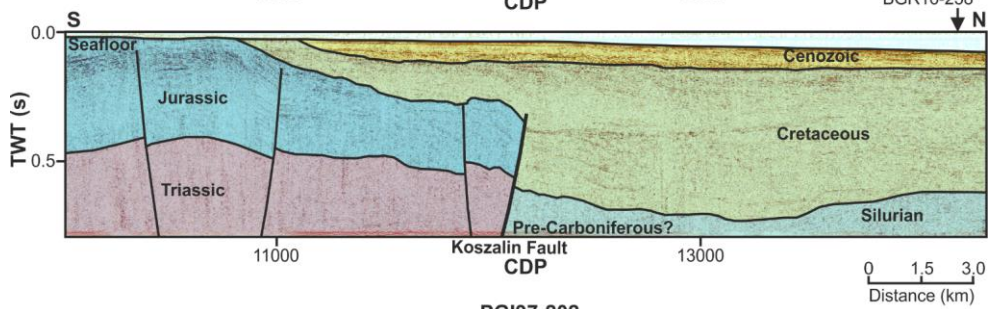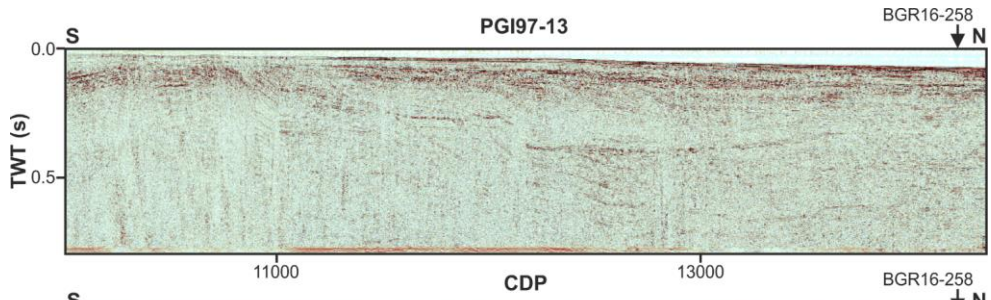
Figure 10~~11~~: Uninterpreted and interpreted PGI97 reprocessed seismic lines PGI97-13 and PGI97-202 (see Fig. 1 for location).

6 Discussion

The foundation for this study was the development of an optimal seismic data processing workflow for the selected BalTec
450 seismic profiles offshore Poland. Due to the acquisition in shallow water environment, our processing strategy focused on suppressing multiple reflections and guided waves, through a cascaded application of SRME, τ-p deconvolution, water bottom F-K filtering, and parabolic Radon multiple elimination. The processing workflow outlined here (with the details provided in the Supplementary Material) could be easily adapted to other multichannel seismic data acquired in the Baltic Sea (or shallow water in general). In order to expand the coverage of the seismic database, we also investigated improving the quality of the
455 legacy PGI97 seismic data using modern processing techniques. While the reprocessed profiles did not contribute significantly to the interpretation presented in our study (mostly because of the original acquisition limitations), post-stack migrated results show significant improvement in overall data quality compared to images from the original processing presented in Krzywiec et al. (2003). On one hand, it confirms the value of revisiting legacy data, on the other hand, the new BalTec data are strikingly better at imaging the geology of the study area (Figure 4).

460 **6.1 Processing of the new BalTec seismic data**

The BalTec processing workflow outlined in section 4.1 focused on removing multiple problems because the data was acquired in a shallow water environment. Figure 4 highlights the main types of noises and multiples existing in the shot and CDP domain. The first demultiple approach used in the processing flow is SRME to suppress the dominant short-path multiples in the shot domain (red arrows in Fig. 4A). These multiples may be peg legs which bounce once or more between the seafloor
465 and the high amplitude reflecting plane below (potentially the top Silurian) (Levin and Shah, 1977), and reverberations of the seafloor and strong reflection events (McGee, 1991). Demultiple techniques such as predictive deconvolution in X-T or τ-p domain and SRME are typically used for removing these short-path multiples (Sheriff and Geldart, 1995; Verschuur, 2013). Given that the SRME was more effective in the deeper part of the shot gather, it was chosen over the predictive deconvolution in this case. More importantly, the SRME method can model all kinds of surface-related multiples including water layer-related
470 multiples and peg-legs (Verschuur et al., 1992, Verschuur, 2013). The shot gather after SRME shows short-path multiples and surface-related multiples successfully suppressed (Fig. 4B), especially at near offset due to the sensitivity of the SRME algorithm in near-offset multiple reconstructions (Qu et al., 2021).

Following the SRME, τ-p deconvolution is another efficient approach for the multiple elimination from the BalTec data. The τ-p deconvolution when performed together with muting in the τ-p domain addressed different types of noise besides multiples,
475 i.e. direct wave, seismic interference, or guided waves (Fig. 4B). The direct waves travel directly from sources to receivers and appear as linear event in the gather (black arrows in Fig. 4B), they are a typical type of noise in any marine seismic dataset. Whereas the guided waves are commonly found in seismic data from shallow water environments and are most recognized in

far offset in the field record (green arrows in Fig. 4B) (Yilmaz, 2001). The guided waves in the shot gather probably represent multiples of the refracted energy. The example of a shot gather after applying τ-p deconvolution (Fig. 4C) and τ-p mute shows a much cleaner gather without these linear coherent noises, and increases the primary event at far offset. The seismic interference (blue arrows in Fig. 4B) was also suppressed by τ-p deconvolution, this type of noise usually happens during a multi-vessel acquisition. In this case, the seismic interference and primary events could be separated in the τ-p transform domain because of their contradicting dips (Gulunay et al., 2004; Elboth et al., 2017).

The example stack sections from line BGR16-202 display a great improvement after the demultiple workflow (Fig. 5). There is noticeable suppression of noise and multiples (black arrows in Fig. 5A). Furthermore, primary events are enhanced to avoid misinterpretation (examples in the oval areas in Fig. 5B). However, the first and second order of the water bottom multiples still exist in the BalTec data stack section (black arrows in Fig. 4C) because it is difficult to predict these events using the SRME algorithm owing to insufficient number of traces in this very shallow water depth area. Therefore, the water bottom F-K filtering approach was applied in the shot domain to eliminate these shallow water bottom multiples. The stack section after this method (Fig. 5D) shows that the dipping primary reflections are no longer interfered with by multiples associated with the water bottom.

The methods based on velocity discrimination might not work properly for the multiples that appeared in the shallow part of the shot and CDP gathers since the move-out difference is not big enough, and the number of traces or samples which are not muted by NMO stretch mute is too sparse. Therefore, in the CDP domain, the high-resolution parabolic Radon demultiple (high-resolution PRT) approach (Harlan, 1995) in the BalTec processing workflow mostly targets the multiples in the deeper part of the CDP gathers (yellow arrows in Fig. 4D) that have larger move-out compared to the primary due to much longer travel time (Hampson, 1986; Sacchi and Ulrych, 1995). The high-resolution PRT approach provided very promising results (Fig. 4E) in cleaning the CDP gather where the NMO-corrected primary events were no longer distracted by large move-out multiples, making velocity picking on such gathers much easier. However, when the data are stacked, there are not that many differences between the data with/without the Radon approach. Removal of these long-path multiples also helps increase signal-to-noise ratios by later stacking process. The cascaded demultiple approach in the BalTec processing workflow improved the velocity analysis as well as helped to produce the final PSTM stack section optimal for subsequent interpretation.

6.2 Reprocessing of the legacy PGI97 data

In case of the PGI97 data, other than the usual linear events that were handled by the F-K filter, the main types of multiples existing in the shot gathers were short-path reverberations and water bottom multiples (Fig. 6B and C). The limited offset of the PGI97 data (~140 m streamer length and 12 channels) (Fig. 2) constrains the application of modern demultiple approaches. Therefore, simple predictive deconvolution (24 ms gap and 300 ms operator length) in the X-T domain is applied to suppress the reverberations. The shot gathers after the predictive deconvolution approach shows noticeable multiples removed,

Two BGR16 profiles show that the CDF is a sharp thrust contact, juxtaposing the Pomeranian Caledonides and the Caledonian
foreland basin (Baltic Basin). This thrust was never reactivated during the subsequent geological history. The profiles do not
contradict the interpretation postulating the thin-skinned character of the Caledonian fold-and-thrust belt (Mazur et al., 2016),
but they do not provide further evidence to confirm this hypothesis. The Caledonian frontal thrust branches off from the
basement slope that may represent a frontal ramp during the end Silurian shortening. However, this cannot be verified because
the top of the Precambrian basement is below the range of seismic imaging (Figs. 68, 79) on the hanging wall of the frontal
overthrust.

The Koszalin Fault was originally formed due to Devonian extensional tectonics. The BGR16-258 profile shows that the fault
was only the north-easternmost one among a number of extensional features downthrowing the top of Silurian toward the SW
(Fig. 79). However, the Koszalin Fault is a structure that marks out the NE limit of this extensional event. Since the late
Palaeozoic tectonic grabens are described along strike onshore Poland and in some other localities of the southern Baltic region
(Krzywiec et al., 2022a and references therein), the Koszalin Fault may belong to a family of structures resulting from a wide-
range tectonic event. This could have been early Carboniferous rifting affecting the passive margin of Laurussia (Smit et al.,
2018), a Middle Devonian continental rifting event (Ponikowska et al., 20243) or a combination of both. Close to the Polish
coast (Figs. 6, 78, 9), and onshore Poland (Mazur et al., 2016), the Koszalin Fault is located SW of the CDF. Therefore, a
narrow zone of the Caledonian basement (Chojnice Structural Zone) is accessible by wells, whereas farther SW, the top

Silurian is downthrown to depths below the interval penetrated by boreholes (Fig. 11a12A). However, farther north, the
540 Koszalin Fault crosses the CDF and cuts through the Precambrian Platform (Fig. 910).

A recent apatite and zircon low-temperature thermochronology study postulates an important early Carboniferous uplift in the
area of the Baltic Basin, NE of the CDF and Koszalin Fault (Botor et al., 2021). It remains uncertain from the seismic profiles
presented whether this uplift was localised along the pre-existing Devonian faults or had a character of long wavelength
doming. The latter possibility seems more likely, observing gradual thinning out of the Carboniferous layer toward the NE
545 (Figs. 68, 79). The domal-style uplift must have persisted until the end of the Permian that is shown by the eastward tapering
of the Zechstein layer (Figs. 68, 79). Therefore, the top Silurian unconformity in the area of the Baltic Basin, earlier considered
a Variscan unconformity, may represent an early Carboniferous uplift event. Furthermore, the original extent of Devonian and
Carboniferous sediments towards the east could be different than today.

The Koszalin Fault was certainly reactivated as a normal dip-slip feature in the Triassic (Fig. 11b12B). More than 1 km of
550 Triassic sediments and several hundred meters of Jurassic were deposited during continuing Mesozoic subsidence (Figs. 68,
79). The thickness of the later eroded Cretaceous sediments remains unconstrained. In the Mesozoic, the Koszalin Fault
focused nearly all subsidence, while other faults were almost inactive (Fig. 68).

During the late Cretaceous-Paleocene basin inversion, the Koszalin Fault was reactivated as a major reverse fault (Fig.
11c12C). The fault limited the eastern limb of the Kołobrzeg anticline and facilitated its uplift exceeding 1 km (Fig. 1). After
555 the activity ceased, the Koszalin Fault was covered by the marginal part of a syntectonic Cretaceous trough, the subsidence of
which lasted longer than the inversion. The onlap of Upper Cretaceous sediments may have been related to the bending of the
anticline crest.
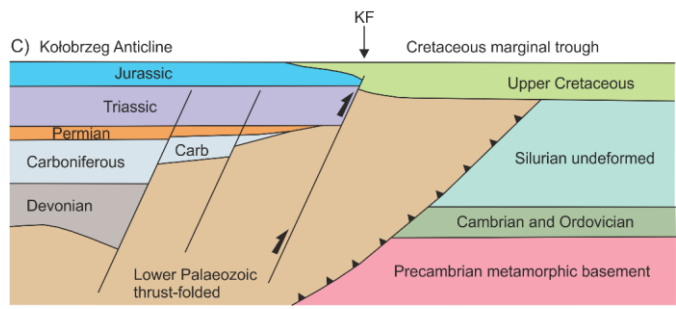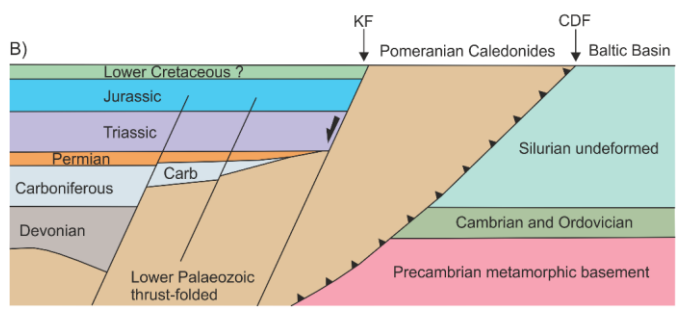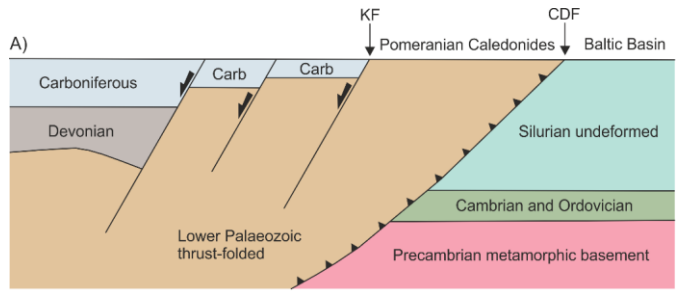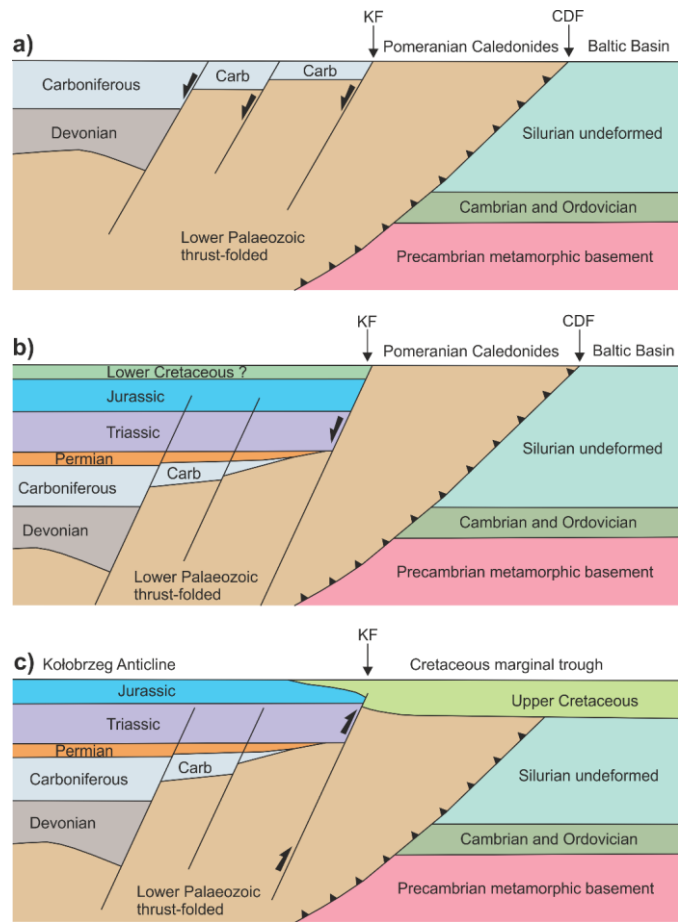
560   **Figure 11~~12~~**: Conceptual diagrams showing tectonic evolution of the transition zone between the Precambrian and Palaeozoic
Platforms offshore Poland for early Carboniferous (~~A~~a), middle Cretaceous (~~B~~b), and post-Paleocene (~~C~~c). ~~A~~a – Deposition
of late Palaeozoic strata west of the Pomeranian Caledonides resulted from normal, dip-slip faulting, initiated in the Middle
Devonian and lasting until the early Carboniferous. ~~B~~b – Permian-Mesozoic extension was focused on the Koszalin Fault

after a period of late early to late Carboniferous uplift, ~~C~~ c – Late Cretaceous-Paleocene inversion formed the Kołobrzeg Anticline and Upper Cretaceous marginal trough.

7 Conclusions

~~In this study, we developed an optimal seismic data processing workflow for the selected BalTec seismic profiles offshore Poland. Due to the acquisition in a shallow water environment, the processing strategy focused on suppressing multiple reflections and guided waves, through a cascaded application of SRME, τ-p deconvolution, Water bottom F-K filtering, and parabolic Radon multiple elimination. The processing workflow presented here could be easily adapted to other multichannel seismic data acquired in the Baltic Sea (or shallow water in general). We also investigated improving the quality of the legacy PGI97 seismic data using modern processing techniques. While the reprocessed profiles did not contribute significantly to the interpretation presented in our study (mostly because of the original acquisition limitations), post-stack migrated results show significant improvement in overall data quality compared to images from the original processing presented in Krzywiec et al. (2003). This in turn confirms the value of revisiting legacy data.~~

~~With the newly processed and reprocessed data, w~~We attempted a new seismic interpretation of the sedimentary successions overlying the crystalline basement in the transition zone from the Precambrian to Palaeozoic Platforms offshore Poland using the new (BalTec), as well as vintage (DBE) and reprocessed legacy reflection seismic data (PGI97). Both processing and reprocessing efforts were developed in-house with a particular emphasis on multiple reflection elimination. Even though the interpretation was hampered by the lack of sufficient well data control, we managed to provide some constraints on the tectonic evolution of the Koszalin Fault and its relation to the CDF.

~~The Koszalin Fault was the main structure controlling Mesozoic subsidence and Late Cretaceous-Paleocene inversion of the eastern portion of the Mid-Polish Trough offshore Poland. The inversion changed its character from thin- to thick-skinned towards the north, away from the Polish coast. The Koszalin Fault reactivated older structural grain inherited from the time of Devonian continental rifting at the margin of Laurussia. The fault runs obliquely to the CDF, the feature that remained inactive since its formation at the Silurian-Devonian transition.~~

The paper discusses geological features in the transition zone between the East European Precambrian Platform and the West European Palaeozoic Platform, focusing on the CDF and the Koszalin Fault. It highlights the CDF as a thrust contact between the Pomeranian Caledonides and the Caledonian foreland basin, suggesting it remained inactive throughout subsequent geological history. The Koszalin Fault originated from Devonian extensional tectonics and may represent a broader tectonic event, related to late Palaeozoic continental rifting and post-rift thermal subsidence. After a period of overall uplift in the Carboniferous and early Permian, the fault experienced reactivation during the Triassic as a normal dip-slip feature. Mesozoic subsidence in the area was primarily focused along the Koszalin Fault, while other faults remained less active. During the Late

595 Cretaceous-Paleocene, the Koszalin Fault became a major reverse fault, influencing basin inversion, growth of inversion-related anticline and formation of the Late Cretaceous syn-inversion marginal through.

Acknowledgements

This study was funded by the Polish National Science Centre grant no UMO-2017/27/B/ST10/02316. S. Stovba thanks the Polish National Science Centre for the Grant UMO-2022/01/3/ST10/00030. Cruise MSM52 has been funded by the German Science Foundation DFG and the Federal Ministry of Education and Research (BMBF). We thank the Federal Institute for Geosciences and Natural Resources (BGR) for their support during seismic data acquisition and sharing of the data. DBE data were provided thanks to the agreement with the Geological Survey of Denmark and Greenland (GEUS).

We would like to thank IHS Markit Ltd. and Petrosys Ltd. for the donation of academic licenses of Kingdom Suite and Globe Claritas software packages, respectively.

We thank the two anonymous reviewers for their helpful comments to improve the manuscript.

Data availability

BalTec (MSM52) seismic data processed in this study are available upon request. PGI97 data are owned by the Polish State Treasury and are available via request from the Polish Ministry of Environment. Danish data are available via request from GEUS.

Author contribution statement

Quang Nguyen: Conceptualization, Methodology, Data Curation, Writing – Original Draft preparation, Software, Visualization. **Michal Malinowski**: Supervision, Project administration, Writing – Review & Editing. **Stanisław Mazur** and **Sergiy Stovba**: Data Curation, Writing – Original Draft preparation. **Małgorzata Ponikowska**: Visualization, Data Curation. **Christian Hübscher**: Project administration, Data provider.

Competing interests

The co-author Michal Malinowski is a member of the editorial board of the Solid Earth journal. The peer-review process was guided by an independent editor, and the authors have also no other competing interests to declare.

References (including the Supplementary Material)

Ahlrichs, N., Hübscher, C., Noack, V., Schnabel, M., Damm, V., Krawczyk, C.M., 2020. Structural Evolution at the Northeast North German Basin Margin: From Initial Triassic Salt Movement to Late Cretaceous-Cenozoic Remobilization. Tectonics 39, e2019TC005927. https://doi.org/10.1029/2019TC005927.

Ahlrichs, N., Noack, V., Hübscher, C., Seidel, E., Warwel, A., Kley, J., 2022. Impact of Late Cretaceous inversion and Cenozoic extension on salt structure growth in the Baltic sector of the North German Basin. Basin Res. 34, 220–250. https://doi.org/10.1111/bre.12617.

Al Hseinat, M., Hübscher, C., 2017. Late Cretaceous to recent tectonic evolution of the North German Basin and the transition zone to the Baltic Shield/southwest Baltic Sea. Tectonophysics 708, 28–55. https://doi.org/10.1016/j.tecto.2017.04.021.

Antonowicz, L., Iwanowska, E. and Rendak, A., 1994. Tensional tectonics in the Pomeranian section of the TT Zone and the implications for hydrocarbon exploration. Geological Quarterly, 38(2), pp.289-306.

Babel Working Group, 1993. Deep Seismic Reflection/Refraction Interpretation of Crustal Structure along Babel Profiles A and B in the Southern Baltic Sea. Geophys. J. Int. 112, 325–343. https://doi.org/10.1111/j.1365-246X.1993.tb01173.x.

Bayer, U., Grad, M., Pharaoh, T.C., Thybo, H., Guterch, A., Banka, D., Lamarche, J., Lassen, A., Lewerenz, B., Scheck, M., Marotta, A.-M., 2002. The southern margin of the East European Craton: new results from seismic sounding and potential fields between the North Sea and Poland. Tectonophysics, Geophysical Investigations og the Trans-European Suture Zone II 360, 301–314. https://doi.org/10.1016/S0040-1951(02)00359-1.

Beier, H. and Katzung, G., 1999. Lithologie und Strukturgeologie des Altpaläozoikums in der Offshore-Bohrung G 14-1/86 (südliche Ostsee). Greifswalder Geowissenschaftliche Beiträge, 6, pp.327-345.

Berthelsen, A., 1998. The Tornquist Zone northwest of the Carpathians: An intraplate pseudosuture. GFF 120, 223–230. https://doi.org/10.1080/11035899801202223.

Botor, D., Mazur, S., Anczkiewicz, A.A., Dunkl, I., Golonka, J., 2021. Thermal history of the East European Platform margin in Poland based on apatite and zircon low-temperature thermochronology. Solid Earth 12, 1899–1930. https://doi.org/10.5194/se-12-1899-2021.

Canales, L.L., 1984. Random noise reduction. In SEG Technical Program Expanded Abstracts 1984 (pp. 525-527). Society of Exploration Geophysicists.

Claerbout, J.F., Doherty, S.M., 1972. Downward continuation of moveout-corrected seismograms. Geophysics 37, 741–768. https://doi.org/10.1190/1.1440298.

Dadlez, R., Narkiewicz, M., Stephenson, R.A., Visser, M.T.M., van Wees, J.-D., 1995. Tectonic evolution of the Mid-Polish Trough: modelling implications and significance for central European geology. Tectonophysics 252, 179–195. https://doi.org/10.1016/0040-1951(95)00104-2.

Dallmeyer, R.D., Giese, U., Glasmacher, U., Pickel, W., 1999. First 40Ar/39Ar age constraints for the Caledonian evolution of the Trans–European Suture Zone in NE Germany. J. Geol. Soc. 156, 279–290. https://doi.org/10.1144/gsjgs.156.2.0279.

DEKORP-BASINResearch Group, 1999. Deep crustal structure of the Northeast German basin: New DEKORP-BASIN '96 deep-profiling results. Geology 27, 55–58. https://doi.org/10.1130/0091-7613(1999)027<0055:DCSOTN>2.3.CO;2.

Elboth, T., Shen, H., Khan, J., 2017. Advances in Seismic Interference Noise Attenuation. Presented at the 79th EAGE Conference and Exhibition 2017, European Association of Geoscientists & Engineers, pp. 1–5. https://doi.org/10.3997/2214-4609.201700579.

Erlström, M., Thomas, S.A., Deeks, N., Sivhed, U., 1997. Structure and tectonic evolution of the Tornquist Zone and adjacent sedimentary basins in Scania and the southern Baltic Sea area. Tectonophysics 271, 191–215. https://doi.org/10.1016/S0040-1951(96)00247-8.

Franke, D., Gründel, J., Lindert, W., Meissner, B., Schulz, E., Zagora, I. and Zagora, K., 1994. Die Ostseebohrung G 14–eine Profilübersicht. Z. geol. Wiss, 22(1-2), pp.235-240.

Gągała, Ł., Vergés, J., Saura, E., Malata, T., Ringenbach, J.-C., Werner, P., Krzywiec, P., 2012. Architecture and orogenic evolution of the northeastern Outer Carpathians from cross-section balancing and forward modelling. Tectonophysics 532–535, 223–241. https://doi.org/10.1016/j.tecto.2012.02.014.

Graversen, O., 2004. Upper Triassic–Lower Cretaceous seismic sequence stratigraphy and basin tectonics at Bornholm, Denmark, Tornquist Zone, NW Europe. Mar. Pet. Geol. 21, 579–612. https://doi.org/10.1016/j.marpetgeo.2003.12.001.

GülünayGulunay, N., Magesan, M., Baldock, S., 2004. Seismic Interference Noise Attenuation. Presented at the 2004 SEG Annual Meeting, OnePetro.

Gülünay, N., 2017. Signal leakage in f-x deconvolution algorithms. Geophysics, 82(5), pp.W31-W45.

Guterch, A., Grad, M., Janik, T., Materzok, R., Luosto, U., Yliniemi, J., Luck, E., Schulze, A., Forste, K., 1994. Crustal structure of the transition zone between Precambrian and Variscan Europe from new seismic data along LT-7 profile (NW Poland and eastern Germany). Comptes Rendus - Acad. Sci. Ser. II Sci. Terre Planetes 319, 1489–1496.

Hampson, D., 1986. Inverse velocity stacking for multiple elimination, in: SEG Technical Program Expanded Abstracts 1986, SEG Technical Program Expanded Abstracts. Society of Exploration Geophysicists, pp. 422–424. https://doi.org/10.1190/1.1893060.

Hansen, M., & Poulsen, V. (1977). Ekskursionsfører nr. 1, Geologi på Bornholm, VARV, København, 96 pp.

Harlan, W.S., 1995. Regularization by model reparameterization. This Website Pap. Pdf.

Hübscher, C., 2018. Geophysical profiles during Maria S. Merian cruise MSM52. Inst. Für Geophys. Univ. Hambg. https://doi.org/10.1594/PANGAEA.890870.

Hübscher, C., Ahlrichs, H., Allum, G., Behrens, T., Bülow, J., Krawczyk, C., Damm, V., Demir, Ü., Engels, M., Frahm, L., Grzyb, G., Hahn, B., Heyde, I., Juhlin, C., Knevels, K., Lange, G., Bruun Lydersen, I., Malinowski, M., Noack, V., Preine, J., Rampersad, K., Schnabel, M., Seidel, E., Sopher, D., Stakemann, Jo. & Stakemann, Ja. (2017). BalTec - Cruise No.MSM52 – March 1 – March 28, 2016 – Rostock (Germany) – Kiel (Germany). MARIA S. MERIAN-Berichte, MSM52, 46 pp. DFGSenatskommission für Ozeanographie. https://doi.org/10.2312/cr_msm52.

Janik, T., Wójcik, D., Ponikowska, M., Mazur, S., Skrzynik, T., Malinowski, M., Hübscher, C., 2022. Crustal structure across the Teisseyre-Tornquist Zone offshore Poland based on a new refraction/wide-angle reflection profile and potential field modelling. Tectonophysics 828, 229271. https://doi.org/10.1016/j.tecto.2022.229271.

Jaworowski, K., Wagner, R., Modliski, Z., Pokorski, J., Sokołowski, J., Sokołowski, A., 2010. Marine ecogeology in semi-closed basin: case study on a threat of geogenic pollution of the southern Baltic Sea (Polish Exclusive Economic Zone). Geol. Q. 54, 267–288.

690   Karnkowski, P.H., Pikulski, L., Wolnowski, T., 2010. Petroleum geology of the Polish part of the Baltic region - an overview. Geol. Q. 54, 143–158.

Katzung, G., 2001. The Caledonides at the southern margin of the East European Craton. Neues Jahrb. Für Geol. Paläontol. - Abh. 3–53. https://doi.org/10.1127/njgpa/222/2001/3.

Katzung, G., Giese, U., Walter, R., Winterfeld, C.V., 1993. The Rügen Caledonides, northeast Germany. Geol. Mag. 130,
695   725–730. https://doi.org/10.1017/S0016756800021038.

Kramarska, R., Krzywiec, P., Dadlez, R., Jegliński, W., Papiernik, B., Przezdziecki, P. and Zientara, P., 1999. Geological map of the Baltic Sea bottom without Quaternary deposits. Panstwowy Instytut Geologiczny, Gdansk-Warszawa.

Krawczyk, C.M., Eilts, F., Lassen, A., Thybo, H., 2002. Seismic evidence of Caledonian deformed crust and uppermost mantle structures in the northern part of the Trans-European Suture Zone, SW Baltic Sea. Tectonophysics, Geophysical
700   Investigations of the Trans-European Suture Zone II 360, 215–244. https://doi.org/10.1016/S0040-1951(02)00355-4.

Krzywiec, P., 2001. Contrasting tectonic and sedimentary history of the central and eastern parts of the Polish Carpathian foredeep basin — results of seismic data interpretation. Mar. Pet. Geol. 18, 13–38. https://doi.org/10.1016/S0264-8172(00)00037-4.

Krzywiec, P., 2002. Mid-Polish Trough inversion – seismic examples, main mechanisms, and its relationship to the
705   Alpine-Carpathian collision. Stephan Mueller Spec. Publ. Ser. 1, 151–165. https://doi.org/10.5194/smsps-1-151-2002.

Krzywiec, P., Kramarska, R., Zientara, P., 2003. Strike-slip tectonics within the SW Baltic Sea and its relationship to the inversion of the Mid-Polish Trough—evidence from high-resolution seismic data. Tectonophysics, Dynamics of Sedimentary Basin Inversion: Observations and Modelling 373, 93–105. https://doi.org/10.1016/S0040-1951(03)00286-5.

710   Krzywiec, P., Kufrasa, M., Poprawa, P., Mazur, S., Koperska, M., Ślemp, P., 2022a. Together but separate: decoupled Variscan (late Carboniferous) and Alpine (Late Cretaceous–Paleogene) inversion tectonics in NW Poland. Solid Earth 13, 639–658. https://doi.org/10.5194/se-13-639-2022.

Krzywiec, P., Oszczypko, N., Bukowski, K., Oszczypko-Clowes, M., Śmigielski, M., Stuart, F.M., Persano, C., Sinclair, H.D., 2014. Structure and evolution of the Carpathian thrust front between Tarnów and Pilzno (Pogórska Wola area, southern
715   Poland): results of integrated analysis of seismic and well data. Geol. Q. Vol. 58, No. 3. https://doi.org/10.7306/gq.1189.

Krzywiec, P., Stachowska, A., Grzybowski, Ł., Nguyen, Q., Słonka, Ł., Malinowski, M., Kramarska, R., Ahlrichs, N., Huebscher, C., 2022b. The Late Cretaceous inversion of the Polish Basin and surrounding area – a current perspective based on seismic data. In: Jagt, J.W.M, Jagt-Yazykova, E., Walaszczyk, I., Żylińska, A. (Eds.), Cretaceous of Poland and of Adjacent Areas, 11th International Cretaceous Symposium. Faculty of Geology, University of Warsaw, Warsaw,
720   Poland. pp. 9–23.

Lassen, A., Thybo, H., Berthelsen, A., 2001. Reflection seismic evidence for Caledonian deformed sediments above Sveconorwegian basement in the southwestern Baltic Sea. Tectonics 20, 268–276. https://doi.org/10.1029/2000TC900028.

Levin, F.K., Shah, P.M., 1977. Peg-leg multiples and dipping reflectors. Geophysics 42, 957–981. https://doi.org/10.1190/1.1440775.

Liboriussen, J., Ashton, P., Tygesen, T., 1987. The tectonic evolution of the Fennoscandian Border Zone in Denmark. Tectonophysics, Compressional Intra-Plate Deformations in the Alpine Foreland 137, 21–29. https://doi.org/10.1016/0040-1951(87)90310-6.

Mazur, S., Mikolajczak, M., Krzywiec, P., Malinowski, M., Buffenmyer, V., Lewandowski, M., 2015. Is the Teisseyre-Tornquist Zone an ancient plate boundary of Baltica? Tectonics 34, 2465–2477. https://doi.org/10.1002/2015TC003934.

Mazur, S., Mikolajczak, M., Krzywiec, P., Malinowski, M., Lewandowski, M., Buffenmyer, V., 2016. Pomeranian Caledonides, NW Poland – A collisional suture or thin-skinned fold-and-thrust belt? Tectonophysics, SI: Crustal seismology 692, 29–43. https://doi.org/10.1016/j.tecto.2016.06.017.

Mazur, S., Scheck-Wenderoth, M., Krzywiec, P., 2005. Different modes of the Late Cretaceous–Early Tertiary inversion in the North German and Polish basins. Int. J. Earth Sci. 94, 782–798. https://doi.org/10.1007/s00531-005-0016-z.

McGee, T.M., 1991. Seismic reverberations and the remote estimation of properties of underwater soils. Int. J. Imaging Syst. Technol. 3, 40–57. https://doi.org/10.1002/ima.1850030107.

Monk, D.J., 1993. Wave-equation multiple suppression using constrained gross-equalization. Geophys. Prospect. 41, 725–736. https://doi.org/10.1111/j.1365-2478.1993.tb00880.x.

Nguyen Q, 2020, Seismic Data Processing Report (BALTEC / MSM52). Institute of Geophysics PAS. https://dspace.igf.edu.pl/xmlui/handle/123456789/112.

Nguyen, Q., Malinowski, M., Kramarska, R., Kaulbarsz, D., Mil, L., Hübscher, C., 2023. Gas - Escape features along the Trzebiatów fault offshore Poland: Evidence for a leaking petroleum system. Mar. Pet. Geol. 156, 106431. https://doi.org/10.1016/j.marpetgeo.2023.106431.

Pan, Y., Seidel, E., Juhlin, C., Hübscher, C., Sopher, D., 2022. Inversion tectonics in the Sorgenfrei–Tornquist Zone: insight from new marine seismic data at the Bornholm Gat, SW Baltic Sea. GFF 144, 71–88. https://doi.org/10.1080/11035897.2022.2071335.

Pharaoh, T.C., 1999. Palaeozoic terranes and their lithospheric boundaries within the Trans-European Suture Zone (TESZ): a review. Tectonophysics 314, 17–41. https://doi.org/10.1016/S0040-1951(99)00235-8.

Pietsch, K. and Krzywiec, P.: Application of seismic methods for hydrocarbon exploration within the Devonian and Carboniferous series of the Western Pomerania (Białogard-Jamno area), Oil and Gas News from Poland, 6, 175–186.

Piske, J., Rasch, H.J., Neumann, E. and Zagora, K., 1994. Geologischer Bau und Entwicklung des Präperms der Insel Rügen und des angrenzenden Seegebietes. Zeitschrift für geologische Wissenschaften, 22, pp.211-226.

Podhalańska, T., Modliński, Z., 2006. Stratygrafia i wykształcenie facjalne osadów ordowiku i syluru strefy Koszalin–Chojnice : podobieństwa i różnice z obszarami zachodniej krawędzi kratonu wschodnioeuropejskiego i Rugii. Pr. Państw. Inst. Geol. T. 186.

Podhalaska, T., Modliski, Z., 2010. Outline of the lithology and depositional features of the lower Paleozoic strata in the Polish part of the Baltic region. Geol. Q. Vol. 54, No 2, 109–121.

Pokorski, J., 2010. Geological section through the lower Paleozoic strata of the Polish part of the Baltic region. Geol. Q. 54, 123–130.

Ponikowska, M., Stovba, S.M., Mazur, S., Malinowski, M., Krzywiec, P., Nguyen, Q., Hübscher, C., 2024~~3~~. Crustal-scale pop-up structure at the junction of two continental-scale deformation zones in the southern Baltic Sea. Tectonics, 43, e2023TC008066. https://doi.org/10.1029/2023TC008066.~~Crustal Structure and Tectonic Evolution of the Southern Baltic Sea Interpreted from Seismic, Gravity and Magnetic Data (preprint). Preprints. https://doi.org/10.22541/essoar.169290552.22013600/v1.~~

Qu, S., Verschuur, E., Zhang, D., Chen, Y., 2021. Training deep networks with only synthetic data: Deep-learning-based near-offset reconstruction for (closed-loop) surface-related multiple estimation on shallow-water field data. Geophysics 86, A39–A43. https://doi.org/10.1190/geo2020-0723.1.

Rempel, H., 1992. Erdölgeologische Bewertung der Arbeiten der Gemeinsamen Organisation Petrobaltic im deutschen Schelfbereich. Geologisches Jahrbuch. Reihe D. Mineralogie, Petrographie, Geochemie, Lagerstättenkunde, (99), pp.3-32.

Sacchi, M.D., Ulrych, T.J., 1995. High-resolution velocity gathers and offset space reconstruction. Geophysics 60, 1169–1177. https://doi.org/10.1190/1.1443845.

Schlüter, H., Best, G., Jürgens, U., Binot, F. 1997. Interpretation reflexionsseismischer Profile zwischen baltischer Kontinentalplatte und kaledonischem Becken in der südlichen Ostsee – erste Ergebnisse. Zeitschrift der deutschen geologischen Gesellschaft, 148, 1–32.

Schlüter, H.U., Jürgens, U., Binot, F. and Best, G., 1998. The importance of geological structures as natural sources of potentially hazardous substances in the southern part of the Baltic Sea. ZEITSCHRIFT FUR ANGEWANDTE GEOLOGIE, 44, pp.26-32.

Seidel, E., Meschede, M., Obst, K., 2018. The Wiek Fault System east of Rügen Island: origin, tectonic phases and its relationship to the Trans-European Suture Zone. Geol. Soc. Lond. Spec. Publ. 469, 59–82. https://doi.org/10.1144/SP469.10.

~~Sheriff, R.E., Geldart, L.P., 1995. Exploration Seismology. Cambridge University Press.~~

Smit, J., van Wees, J.-D., Cloetingh, S., 2018. Early Carboniferous extension in East Avalonia: 350 My record of lithospheric memory. Mar. Pet. Geol. 92, 1010–1027. https://doi.org/10.1016/j.marpetgeo.2018.01.004.

Sopher, D., Erlström, M., Bell, N., Juhlin, C., 2016. The structure and stratigraphy of the sedimentary succession in the Swedish sector of the Baltic Basin: New insights from vintage 2D marine seismic data. Tectonophysics 676, 90–111. https://doi.org/10.1016/j.tecto.2016.03.012.

Stoffa, P.L., Diebold, J.B., Buhl, P., 1981. Inversion of seismic data in the τ-p plane. Geophys. Res. Lett. 8, 869–872. https://doi.org/10.1029/GL008i008p00869.

Thomas, S.A., Sivhed, U., Erlström, M., Seifert, M., 1993. Seismostratigraphy and structural framework of the SW Baltic Sea. Terra Nova 5, 364–374. https://doi.org/10.1111/j.1365-3121.1993.tb00270.x.

Thybo, H., 1999. Crustal structure and tectonic evolution of the Tornquist Fan region as revealed by geophysical methods. Bull. Geol. Soc. Den. 46. https://doi.org/10.37570/bgsd-1999-46-12.

Thybo, H., 2001. Crustal structure along the EGT profile across the Tornquist Fan interpreted from seismic, gravity and magnetic data. Tectonophysics 334, 155–190. https://doi.org/10.1016/S0040-1951(01)00055-5.

Torsvik, T.H., Rehnström, E.F., 2003. The Tornquist Sea and Baltica–Avalonia docking. Tectonophysics, Paleomagnetism Applied to Tectonics. A tribute to Rob Van der Voo 362, 67–82. https://doi.org/10.1016/S0040-1951(02)00631-5.

van Wees, J.-D., Stephenson, R.A., Ziegler, P.A., Bayer, U., McCann, T., Dadlez, R., Gaupp, R., Narkiewicz, M., Bitzer, F., Scheck, M., 2000. On the origin of the Southern Permian Basin, Central Europe. Mar. Pet. Geol. 17, 43–59. https://doi.org/10.1016/S0264-8172(99)00052-5.

Vejbaek, O.V., Stouge, S., Damtoft Poulsen, K., 1994. Palaeozoic tectonic and sedimentary evolution and hydrocarbon prospectivity in the Bornholm area.

Verschuur, D.J., 2013. Seismic Multiple Removal Techniques: Past, present and future (EET 1). Earthdoc. https://doi.org/10.3997/9789073834965.

Verschuur, D.J., Berkhout, A.J., Wapenaar, C.P.A., 1992. Adaptive surface-related multiple elimination. Geophysics 57, 1166–1177. https://doi.org/10.1190/1.1443330.

Wang, Y., 2003. Multiple subtraction using an expanded multichannel matching filter. Geophysics 68, 346–354. https://doi.org/10.1190/1.1543220.

Weglein, A.B., 1999. Multiple attenuation: an overview of recent advances and the road ahead (1999). Lead. Edge 18, 40–44. https://doi.org/10.1190/1.1438150.

Yilmaz, Ö., 2001. Seismic Data Analysis: Processing, Inversion, and Interpretation of Seismic Data. Society of Exploration Geophysicists. https://doi.org/10.1190/1.9781560801580.

Zhou, B., Greenhalgh, S.A., 1994. Linear and parabolic tau -p transforms revisited. Geophysics 59, 1133–1149. https://doi.org/10.1190/1.1443669.